AUS DEM LEHRSTUHL
FÜR MEDIZINISCHE MIKROBIOLOGIE UND HYGIENE
PROF. DR. DR. ANDRÉ GESSNER
DER FAKULTÄT FÜR MEDIZIN
DER UNIVERSITÄT REGENSURG

IN VITRO DIFFERENTIATION OF GENOME ENGINEERED STEM CELLS FOR A NOVEL HIV THERAPY

Inaugural – Dissertation
zur Erlangung des Doktorgrades
der Medizin

der
Fakultät für Medizin
der Universität Regensburg

vorgelegt von
Sebastian Benedikt Hoffmann

2019

AUS DEM LEHRSTUHL
FÜR MEDIZINISCHE MIKROBIOLOGIE UND HYGIENE
PROF. DR. DR. ANDRÉ GESSNER
DER FAKULTÄT FÜR MEDIZIN
DER UNIVERSITÄT REGENSURG

IN VITRO DIFFERENTIATION OF GENOME ENGINEERED STEM CELLS FOR A NOVEL HIV THERAPY

Inaugural – Dissertation
zur Erlangung des Doktorgrades
der Medizin

der
Fakultät für Medizin
der Universität Regensburg

vorgelegt von
Sebastian Benedikt Hoffmann

2019

Dekan:	Prof. Dr. Dr. Torsten E. Reichert
1. Berichterstatter:	Prof. Dr. Ralf Wagner
2. Berichterstatter:	Prof. Dr. Toni Cathomen

Die Arbeit ist entstanden in der Arbeitsgruppe von Frau Dr. Tatjana Cornu.

Tag der mündlichen Prüfung: 29. Oktober 2019

Table of contents

INTRODUCTION

1.1 CHARACTERISTICS OF HIV AND EPIDEMIOLOGICAL OVERVIEW

The human immunodeficiency virus is an enveloped single strand positive-sense RNA virus with a diameter of 110 nm. It belongs to the subgroup of lentiviridae in the family of retroviridae (1).

There are two major types of HIV: HIV-1 and HIV-2. HIV originally stems from the simian immunodeficiency virus (SIV) which is found especially in chimpanzees. HIV-1 was passed on to the human species from apes while HIV-2 descend from sooty mangabey monkeys (2).

HIV-1 is divided in subgroups such as –M,-N,-O and –P. These subgroups are divided into subtypes. Group –M, the most pandemic subgroup, is composed of subtypes A to D, F to H and J to K (3). This high genetic variability is caused by the recombination and mutation of the reverse transcriptase (4), certainly one of the key-enzymes of HIV.

At the beginning of the 21st century about 49% of all patients worldwide were diagnosed with subtype C. Subtypes A and B caused 12% and 11% of all global infections (4).

In the year 2017 36.9 million people were globally infected with HIV, the infection rate was 2.1 million, and 1.1 million deaths caused by HIV were documented. Recently only about 50% of all infected patients are undergoing therapy. The infection rate as well as the prevalence of HIV could likely be reduced if the remaining 50% (17 million) would undergo antiretroviral therapy, too (5).

The Robert Koch Institute estimated the infection rate to be as high as 2700 patients at the end of 2017 in Germany. It was estimated that 86,100 people were infected of which approximately 11,400 were not diagnosed. Deaths related to HIV (450 in 2017) could be decreased if more infected individuals received treatment. Further a more effective HIV-therapy is highly desirable (6).

An important factor is also the prevention of novel HIV infections as most HIV-positives are infected by unsafe sex practices. A greater knowledge about safe sex and its importance to prevent sexual transmitted diseases needs to be established worldwide (7).

1.2 INFECTION AND VIRUS REPLICATION

In order to spread in the organism, HIV has to enter specific cells to replicate itself. As indicated above, semen and mucosal fluids are the main factors to pass HIV on. $CD4^+$ T-cells, dendritic cells and macrophages are the commonly targeted cells also found in these fluids. Viral entry is mediated by fusion with the cell membrane. For this process the main cellular receptor glycoprotein CD4 as well as one of the chemokine co-receptors CCR5 or CXCR4 on the target cells are required (8) (9). The viral mediator for cell entrance is the surface glycoprotein gp120 together with gp41, a transmembrane protein. The viral tropism defines the strains. The T-tropic strain targets T cells and needs the chemokine co-receptor CXCR4 to enter a T cell. The M-tropic strain targets T cells and macrophages and uses CCR5 as co-receptor.

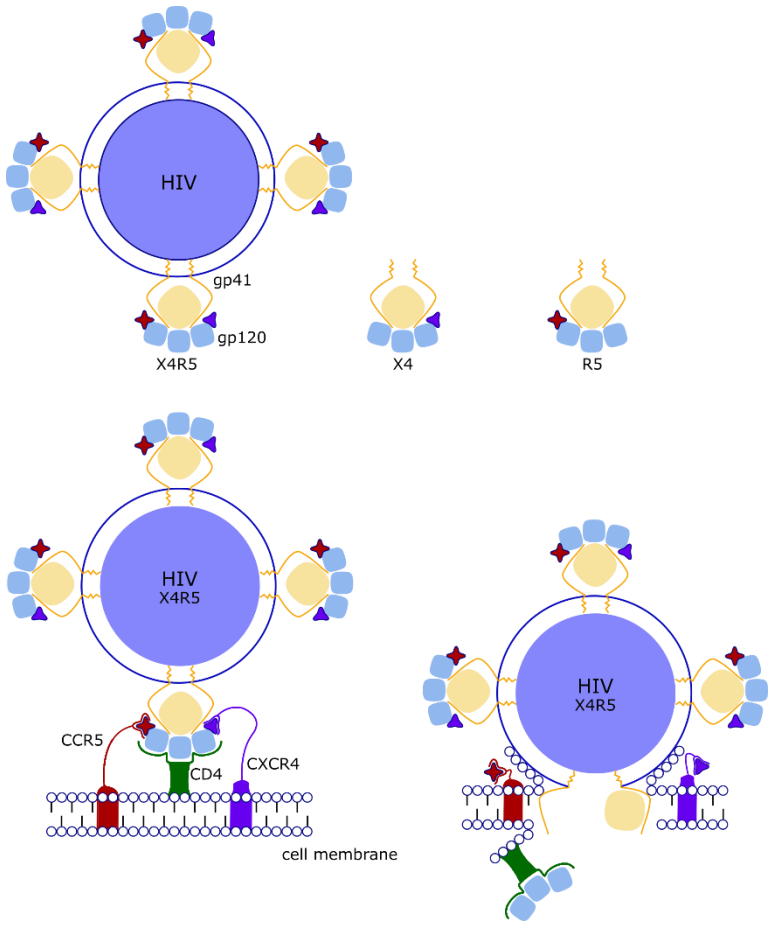

Figure 1: HIV Strains and HIV entry. Three HIV tropisms are shown: the X4R5- mixed tropic virus, the X4-tropic and the R5-tropic virus. Once connected with the target cells the viral membrane fuses with the cell membrane and the viral load is transferred.

There are three kind of virus tropisms: R5-tropism, X4- tropism and dual X4R5-tropism where the virus is able to use both co-receptors (see Figure 1) (10). R5-strains are typically observed in early infection stages (11)(12). Later in the course of the disease a class switch from R5 strain to X4 strain is possible (13).

1.3 DELTA 32 DELETION

About 10% of the northern European population carry a mutation on one CCR5 allele, the so called delta 32 mutation. Between the Baltic and the White Sea a frequency up to 15% is reported (14). Individuals with the delta 32 mutation hold a deletion of 32 bp, nt 554 to 585 in the open reading frame (ORF). The mutation is located in the CKR-5 allele on the short arm of chromosome 3. This deletion is located in a region which codes for the second extracellular loop of the chemokine co-receptor (see Figure 2) The delta 32 mutation introduces a premature stop codon; instead of 352 amino acids (aa) the truncated form has only 215 aa and therefore the CCR5 co-receptor cannot be transported to the cell surface. Individuals with this mutation show a delayed progression of infection if heterozygous. Moreover they are also immune to HIV R5 infection if homozygous for the mutation: it was shown that a group of people carrying the mutation and exposed to HIV were not infected (15).

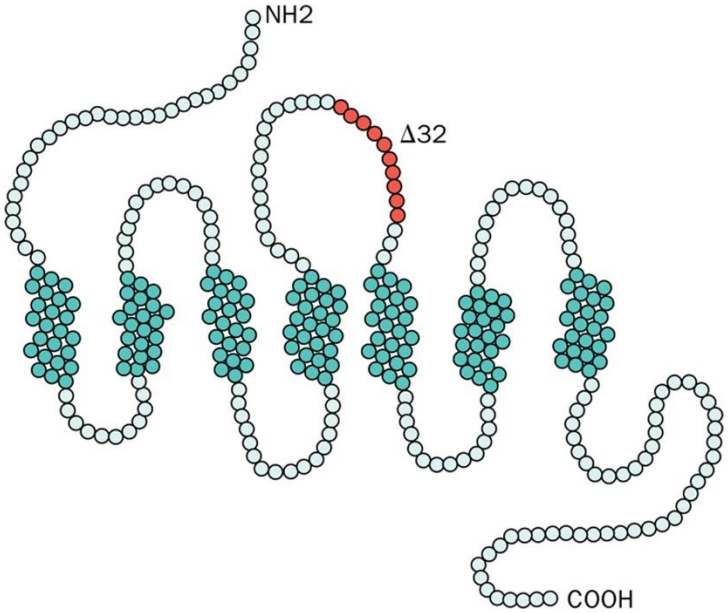

Figure 2: Schematic picture of the CCR5 co-receptor. The amino acids affected by the Δ32 mutation are highlighted in red in the second extracellular loop of the 7-transmembrane-domain-receptor. Graphic modified from Quillent et. al. (16)

1.4 CLASSICAL HIV THERAPY

The classical clinical approach for the treatment of HIV is the -active-retroviral therapy (ART). More than 25 antiretroviral drugs depending on 6 different mechanistic classes are frequently used.

Some antiviral drugs are protease inhibitors (PIs) while others inhibit the proteolytic production of viral proteins fusion inhibitors (FIs) limit the viral invasion to human cells and integrase strand transfer inhibitors (INSTIs) minimize the number of viral DNA integrated to the human genome. Nucleosidic/nucleotidic reverse transcriptase inhibitors (NRTIs/NtRTIs) and non-nucleosidic reverse transcriptase inhibitors (NNRTIs) inhibit the reverse transcription of viral RNA directly to prevent the integration of viral genetic make-up into the human genome. CCR5-Inhibitors prohibit the entrance of HIV into its target cells. Finally there are additionally supportive drugs used to enhance the mechanisms listed above (17) (18).

A big disadvantage of the traditional HIV therapy are the highly abundant side effects. Those are gastrointestinal symptoms such as diarrhea, nausea and vomiting; but also severe side effects such as hepatotoxicity, depressions and suicidality (18). Additionally HIV infection cannot be cured by

ART. In fact, only the progression is delayed. The patient remain infected although the viral load can drop under detection limit.

The first time a patient was declared healed from HIV was “the Berlin patient”. In February 2007 an HIV positive patient suffering from a myeloid leukemia was transplanted with an allogenic haematopoetic stem cell graft by the team of G. Hütter at the Charité hospital in Berlin. For the allogenic transplantation (treatment of the myeloid leukemia) a matched donor homozygous for the Δ32 mutation was chosen, in order to treat the leukemia and render the patient resistant to HIV. After stopping ART on the first day of transplantation, the number of viral RNA-copies showed a long term suppression. Over the years the second main diagnostic marker, the $CD4^+$ T cell surface marker, increased too (19). Usually proviral DNA can be still extracted from the blood and also from tissue of patients who show a long term remission. Under ART therapy reservoirs such as the rectum remain infected by the virus (20). The Berlin patient underwent numerous tests such as single copy assays, apheresis of large amounts of leukocytes from peripheral blood, microdissection of tissues, rectal-biopsy and monitoring of HIV antibodies (19) (21) (22). Nevertheless as of today, the Berlin patient remains virus free in terms of RNA copies as well as in terms of proviral DNA. This approach - the only known curative treatment - is difficult to reproduce on the grounds that Δ32 homozygous donors are scarce: only about 1% of the Caucasian population is homozygous and secondly HLA-matching declines the number of potential donors for transplantation (19).

1.5 GENOMIC ENGINEERING

The key idea of genomic engineering is to modify the human genome. This modification can either be a deletion of nucleotides or an insertion of one or more new nucleotides. Both changes lead to a different genetic code. As many diseases result of only small mutations in the genetic code, genome engineering has great potential to remove those mutations and to provide a cure for hereditary as well as some infectious diseases.

Genomic engineering was first attempted in 1988 with HO endonucleases in order to boost homologous repair in yeast. Endonucleases are enzymes that are able to cleave DNA at specific regions within the two strands. Today there are more specific and more efficient tools than HO

endonucleases. These tools can be designed and customized for any genetic region. The first of these tools were zinc-finger-nucleases (ZFN), followed by transcription-activator-like effector nucleases (TALEN) and lately CRISPR/Cas9 were established (23).

Removing nucleotides leads to a gap in the DNA which would prevent further cell replication. To circumvent cell death, the cells can activate two repair mechanisms which can fix DNA breaks in the genome. These are the non-homologous end joining (NHEJ) and the homologous recombination (HR). Contrary to the HR, NHEJ does not restore the original information and leads to the introduction of small insertions or deletes nucleotides, called InDels. This repair pathway allows to knockout genes which are desired to be silenced. HR restores information relying on the sister chromatid. The redundancy of two identical chromatids prevents the cells from damage due to the lack of genetic information. HR can be used to insert new sequences while introducing a donor DNA template (24) (25).

ZFN consist of 3-6 zinc-finger modules, each of which is able to recognize 3 nucleotides located at the target site. These modules are linked to a FokI domain which set the DNA break and works as a dimer. This type II restriction endonuclease was isolated from Flavobacterium okeanokiotes. Type II restriction enzymes cut DNA closely to their binding sequence. ZFN work as dimers, each unit binds one DNA strand. The binding is necessary for the Fok domains to dimerize and to set a double strand break (DSB) (see Figure 3) (26) (27).

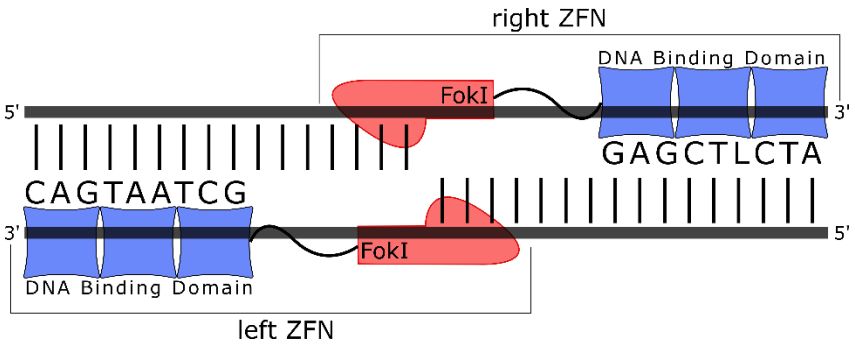

Figure 3: Structure of ZFN. Two ZFNs dimerize to a functional complex. The binding domains built of three zinc-finger modules are designed specifically for the desired locus.

More simple in production, and also less cytotoxic than ZFN are TALEN. Additionally, TALEN are less active in terms of off-target activity if designed for the same sequences (28). Similar to ZFN, TALEN have to dimerize for successful cleavage. Each TALEN consist of a DNA binding

domain, a TALE, that binds to a specific target site and which is linked to the FokI domain (see Figure 4) (25). TALEs have been first discovered in 2006. These effector protein are used by Xanthomonas to overtake the transcriptional machinery of rice plants. They mimick the plants transcriptional factors and facilitate the bacterial infection (29). In 2009 Boch et al. managed to make TAL-III effectors useful for biotechnological purposes. By understanding the genetic code of these proteins they established the knowledge how to design TALEs for specific DNA targeting. The DNA recognition boxes of TALEs in Xanthomonas consist a span of 15.5 to 19.5 repeat domains, while most of them contain 17.5 repeats. A di-amino acid motif on position 12 and 13 interacts directly with DNA bases and is crucial for the sufficient binding of the protein. Nevertheless each repeat corresponds to a certain nucleotide. Due to this mechanism the TALENs' binding domain is very specific to its individual DNA locus (30).

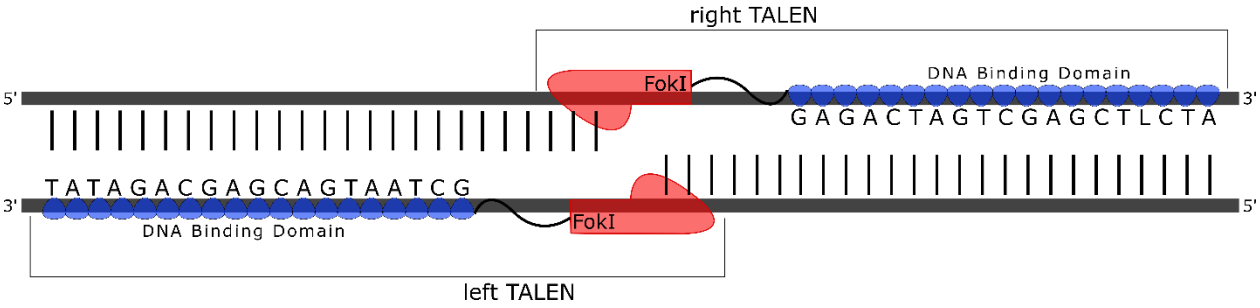

Figure 4: Structure of TALEN. Left and right arm bind to their specific target sequences. Simultaneously the FokI domains dimerize and create a DSB. The binding domain consists of 19 repeat domains with each of them binding to one nucleotide.

With ZFN about 50% of CCR5 disruption can be realized. Perez et al. showed that genetically modified T-cells have a relative survival advantage in contrast to native T-cells whilst challenging with CCR5-tropic HIV-1 in vitro (31). Pablo Tebas et al. showed already in a first clinical study that the gene therapy with ZFN of patients with aviremic HIV infection showed some functionality while reducing the viral load under ART interruption (although the effect was limited) but also safe (32).

E. Meyer in the Cornu Lab showed that using TALEN the cleavage efficiency in $CD34^+$ stem cells derived from cord blood reaches up to nearly 90% on the CCR5 locus. Meyer demonstrated that off-target effects on CCR2, which is a locus highly similar to CCR5, were below background, whereas in the ZFN setting the off-target on the CCR2 locus were significant (33).

In the present study, the used pair of TALEN bind and cleave directly beyond the sequence coding for N-terminus of the CCR5 protein. The region located in this area containing several tyrosine is known to be crucial for HIV binding into the target cells (34). The disruption of this important part of CCR5 should prevent HIV from entering and the chances to create HIV resistant cells are increased.

1.6 T CELL DEVELOPMENT

T cell development in-vivo.

Different premature T cells develop from the common lymphoid progenitor. These premature T cells migrate from the bone marrow to the thymus where differentiation takes place. *In-vivo* the process of differentiation takes three to four weeks (see Figure 5). Lymphopoetic stem cells in the thymus are called thymocytes or thymus-dependent T-lymphocytes. After differentiation the cells undergo a stage of high proliferation. Ligands interacting with Notch 1 receptor and IL-7 then drive the thymocytes towards the T cell lineage. At the beginning the $CD4^-$ /$CD8^-$, so called double negative thymocytes (DN), are generated. The DN rearrange their T cell receptor genes during the β-selection. A broad variability of different T cells is created in order to defend the organism against a maximum number of different pathogens. Thymocytes that have not rearranged the TCR β-chain undergo apoptosis (35).

A minority of these precursor T cell will be part of the γδ-lineage whilst the majority will become part of the αβ-lineage. As the expressed Pre-T cell receptor and CD3 build a complex the T cell precursors are now $CD3^+$. The γδ-T cells remain $CD4^-$ and $CD8^-$ (but $CD3^+$) and they are immediately exported to the periphery. αβ-T cells migrate to the thymic cortex where they become $CD4^+$ and $CD8^+$ double positive cells and subsequently move back to the medulla.

The early T cell receptor is able to recognize self-antigens presented on MHC molecules by the thymic epithelium. Selections guarantee that the mature T cells will be able to efficiently defeat a wide array of pathogens while not attacking cells from the own organism. First the cells undergo a positive selection; they slightly bind the MHC molecules and receive a “surviving signal” - all cells which bind too strongly or too weakly do not survive. In the second selection process, a negative selection, thymocytes that bind too strongly on self-antigens undergo apoptosis. The remaining

cells either become $CD4^+$ or $CD8^+$ single positive depending on their interaction with MHC-I or MHC-II and they are sent as mature T cells to the periphery (35,36).

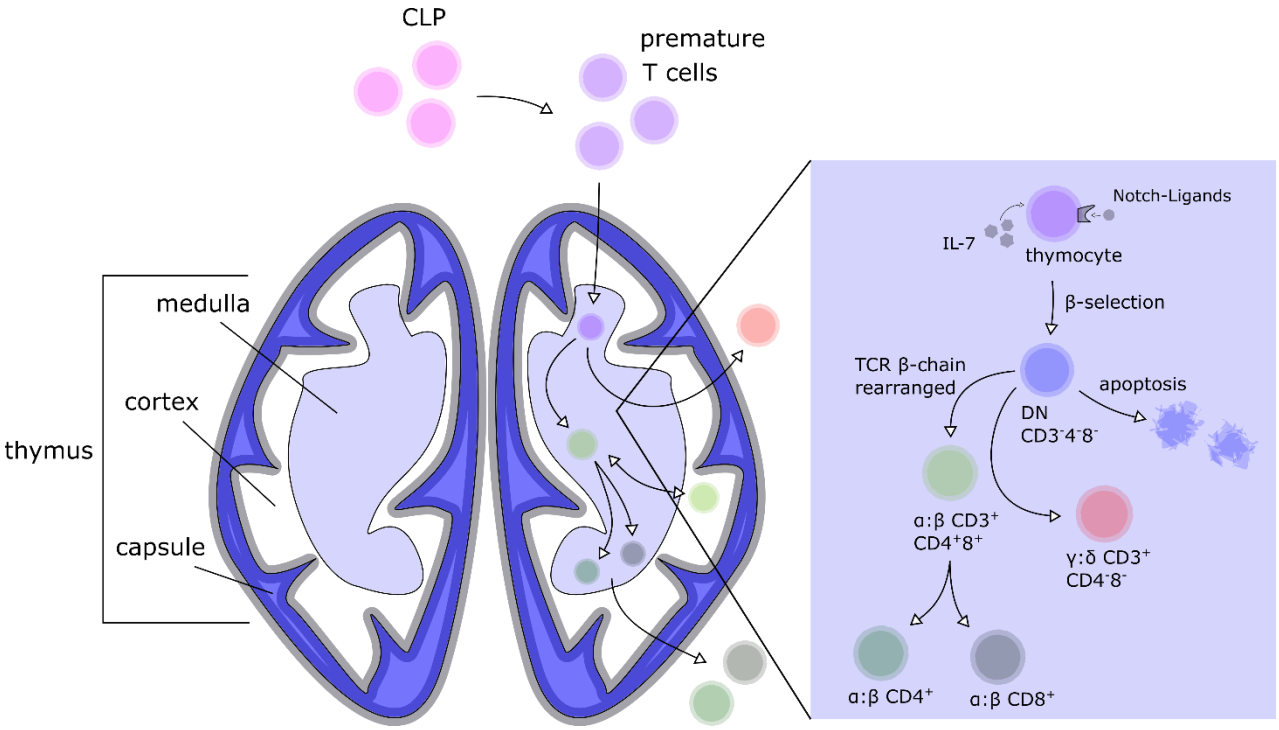

Figure 5: Schematic view of the differentiation process of T cells *in-vivo*. Common lymphoid progenitor (CLP) cells differentiate into premature T cells. These cells migrate from the bone marrow to the thymic medulla where they differentiate under the influence of IL-7 and Notch ligands further and finally undergo β-selection. DN cells which are not able to rearrange their TCR β -chain die. γδ-T cells are immediately exported to the periphery while αβ-T cells move to the cortex. After reaching a $CD4^+8^+$ double positive state they lose one of these trades, move back to the medulla and then undergo a second process of selection. At the end of differentiation mature T cells either $CD4^+$ or $CD8^+$ are exported to the periphery. Graphic modified from Janeway's Immunology (35).

T cell development in-vitro.

Haematopoietic stem cells (HSC) are multipotent. Both the myeloid as well as the lymphoid cell lineage develop from HSCs. These stem cells are $CD34^+$ and can be easily identified by their CD markers. Apart from the bone marrow, the umbilical cord can be used as a source of $CD34^+$ stem cells, too. Contrary to the extraction from bone marrow, the preparation of HSCs from cord blood is less complex and also entails no risks or discomfort for the donor. $CD34^+$ stem cells from cord blood are perfectly suitable for the *in-vitro* differentiation of T cells. (37)

The thymus stroma is absent in an *in-vitro* cell culture setting. OP9-DL1 cells are stromal cells which derive from the bone-marrow. This cell line ectopically expresses the delta-like-1 ligand

which is essential for the Notch signalling pathway (38). OP9-DL1 cells are used as feeder cells and are co-cultured with the T cell precursors to mimic the thymic tissue. Mammals have four different notch receptors. Ligands binding to these receptors are either from the Delta or from the Jagged/Serrate family. The receptors consist of a large type I transmembrane protein. By proteolytic conformational change of the intracellular receptor part an active form is created as soon as a ligand binds to the extracellular part. The whole receptor is translocated to the nucleus where it influences CBF1/RBP-J_K which is a transcriptional repressor (39) (40). Notch signalling has influence on many different cell types. In haematopoietic cells during haematopoiesis this pathway drives proliferation rather than differentiation. In lymphoid progenitors Notch prevents B-Cell differentiation and strongly supports T cell development (41).

Apart from Notch signalling, IL-7 has to be supplemented to the T cells. IL-7 is known as an important cytokine for differentiation of the lymphoid lineage such as for example natural killer cells (42). Hübner et al. have successfully used this ligand for T cell differentiation (43).

Even before T cell receptor-up-regulation, the cells become sensitive to IL-2 which promotes further proliferation. It is known to be the most important cytokine in terms of T cell proliferation (35). Therefore IL-2 should be added to the cells as soon as double positive (DP) cells are detected.

The different subsets of premature T cells can be pinpointed via flow cytometry. The cluster of differentiation (CD) markers are up- and downregulated depending on the differentiation stages of the premature T cells. There are four stages that can be described: early T cell progenitors (ETP), T cell progenitors (pro T cells), premature T cells (pre T cells) and immature single positive T cells (ISP). With the help of the CD markers the stage of each T cell progenitors can be determined.

Table 1 describes the phenotypes of T cell precursors. ETPs express $CD34^+$ on their surface, but not yet CD7. Neither CD1α nor CD5 can be found. Pro T cells in contrast already express CD7 while CD34 can still be detected on their surface. Although they are negative for CD1α, their CD5 status is positive. Double positive in terms of CD1α and CD5 are found in pre T cells which keep this phenotype as they become ISP or double positive (CD4/CD8) cells. Their CD34 status is negative, but CD7 is highly expressed. ISP and DP are negative for CD34, but low positive for CD7 (see Table 1) (44)(45).

	ETP	Pro T cells	Pre T cells	ISP/DP
CD34	+	+	-	-
CD7	-	+	+	low
CD5	-	+	+	+
CD1α	-	-	+	+
CD4	-	-	-	+/-
CD8	-	-	-	+/-

Table 1: Phenotype of the four different T cell progenitor subsets.

1.7 MONOCYTE/ MACROPHAGE DEVELOPMENT

Monocyte development in vivo

Monocytes spend about 12-24 hours in the blood stream until they migrate to different types of tissue. In the tissue monocytes differentiate further to macrophages; the "scavengers" (phagocytes) of the immune systems. Phagocytes opsonize pathogens and cell debris: pathogens are incorporated into the cells and then neutralized via digestion. Furthermore, macrophages release cytokines which activate other leucocytes and enhance inflammation. Macrophages play an essential role in both the innate immune response and the subsequent adaptive immune response (35,36).

Stem cells in the bone marrow differentiate firstly in common myeloid progenitors and then later into monoblasts and premonocytes. This process is mainly triggered by a cytokine called macrophage colony stimulating factor (M-CSF). Additionally, IL-3 secreted by TH_1 cells promotes the macrophage evolution too. The complete differentiation in adult monocytes lasts only two days *in-vivo* (see Figure 6) (26, 27).

Adult monocytes express CD14 on their surface. CD14 can be detected on 40-65% of all monocytes and can be considered as a general marker. Additionally to CD14, CD16 can be expressed too. Generally two subsets of monocytes can be distinguished: $CD16^-$ and $CD16^+$ monocytes which have a lower anti-inflammatory potential. In conclusion, CD16 is not highly distinctive for monocytes in general, but defining for subsets of these cells (46).

CD33 is a marker found on osteoclasts and monocytes. Taken alone it is not specific for monocytes, but in combination with CD14, CD33 becomes specific for mononuclear cells. The reason for this

is that osteoclasts are merged cells, so called syncytia. After merging, the "new" cell loses CD14 and the marker can no longer be detected on the surface. A combinatory detection of CD14 and CD33 is therefore a valid assay to proof the presence of monocytes or macrophages (which as well show co-expression of CD14/CD33) (47).

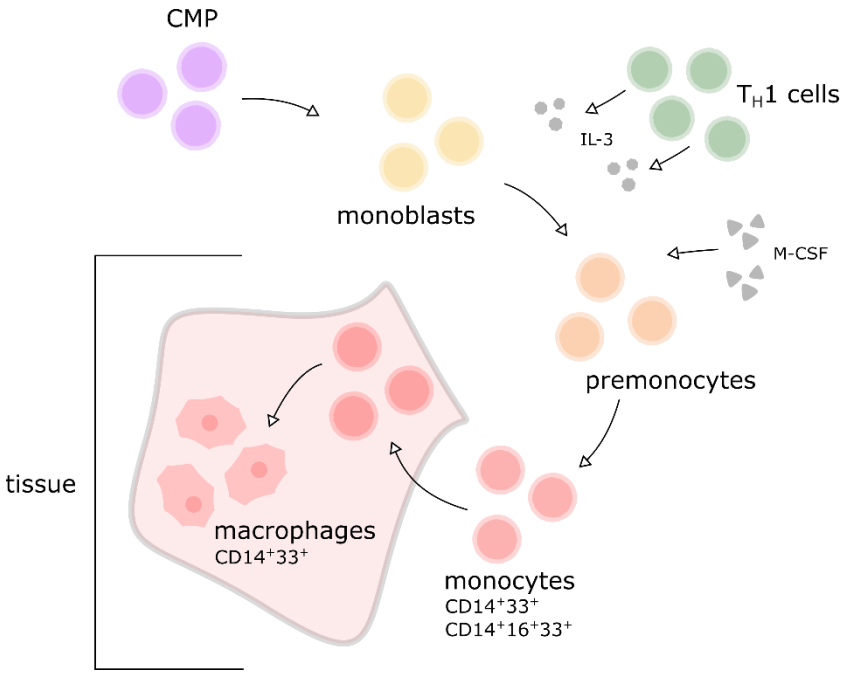

Figure 6: Schematic view of the differentiation process of monocytes *in-vivo*. Common myeloid progenitor (CMP) cells differentiate into monoblasts. Under the influence of IL-3 secreted from T_H1 cells and M-CSF monoblasts differentiate into premonocytes and then into monocytes. Once migrated to the tissue the monocytes finally become macrophages. Macrophages are $CD14^+33^+$. Some monocytes are additionally to CD14 and CD33 also positive for CD16 (35).

Monocyte development in vitro

In-vitro differentiation of $CD34^+$ cord blood derived cells to monocytes/macrophages requires two cytokines: M-CSF and IL-3. M-CSF is found to promote the differentiation from precursor cells into $CD14^+$ macrophages, but inhibits dendritic cell development. The inhibitory effect on dendritic cell differentiation cannot be reversed anymore after only 12 days of M-CSF influence on myeloid precursor cells (48). IL-3 allows the differentiation of monocytes into macrophages. In contrast to M-CSF, a medium containing IL-3 alone is capable of generating dendritic cells. In cultures containing M-CSF and IL-3 both cytokines work synergistic on macrophage differentiation. This condition has, however, not the potential to differentiate dendritic cells (49).

AIM

2.1 PROJECT GOALS

Ideally, targeting CCR5 in $CD34^+$ stem cells would be a "single shot" treatment that causes lifelong protection against HIV R5 tropic strains. If engrafted in the patient, the differentiated target cells would have a survival advantage to the unmodified equivalents. The patient would enrich *in-vivo* HIV resistant cells, because the HIV susceptible cells will be slowly eliminated by the virus. The fundament of the HIV infection was destructed in this way: all target cells, in particular $CD4^+$ cells such as macrophages and T cells, could no longer be infected with R5 tropic strain. This highly innovative therapy concept is the aim at the Institute for Transfusion Medicine and Gene Therapy. A Phase I/II clinical trial is planned and will be carried out soon.

Therefore, I want to demonstrate in our proof of concept and pre-clinical validations that genetically modified human stem cells can develop normally in the preferential HIV target cells: T cell precursors as well as monocytes and pre-stage macrophages. The cells need to go through all differentiation stages found during physiological cell development as indicated above. Furthermore, in unedited samples, I will be monitoring the expression of CCR5 during T cells and monocytes differentiation. This will give an indication in which stage the CCR5 co-receptor emerges in the differentiation process. Also, the earliest stages for an HIV infection of T-cells and monocytes will be determined. Finally CCR5 expression level needs to remain repressed after successfully disrupting the CCR5 gene on the genomic level.

For a clinical approach more data is necessary to be sure that *ex-vivo* modified cells can undergo the normal differentiation process when they are back in vivo.

In the beginning of this thesis, general protocols for the differentiation from $CD34^+$ stem cells derived from cord-blood to monocytes/macrophages and T cells will be established. After setting up a protocol for in vitro differentiation, TALEN treated stem cells are expected to undergo the same process of differentiation as untreated cells. Both treated and untreated cells are then compared and the potential of TALEN treated cells to become mature cells can be evaluated. The immature cells are analysed on their genotype via molecular biologic methods in the course of differentiation. Additionally to the genotype, their phenotype is determined via flow cytometry during the whole process.

MATERIAL AND METHODS

3.1 LINEARIZATION OF DNA PLASMIDS FOR MRNA PRODUCTION

For the mRNA production linearized plasmids were required. TALEN need to dimerize at the target side so a “left” and a “right” protein is needed. The two plasmids that were used for translation are #1539 and #1540.

Both plasmids contain a T7 promoter for the T7 RNA polymerase which is used for mRNA production. After the T7 promoter, the transcription start and the open reading frame (ORF) of the TAL effector DNA binding domain are coded and the FokI cleavage domain follows at the C-terminus.

Plasmid #1539 and #1540 were provided by Cellectis, Paris in the frame of a collaboration.

For the linearization, 10µg of one plasmid was incubated at 37°C for 2 hours together with 2µl Hind III HF (NEB, Germany) and 5µl Cutsmart buffer (NEB, Germany). The solution was filled up to 50µl with RNAse free water (Ambion).

For experimental control, the linearized plasmids were loaded on a 1% agarose gel (see formula below).

3.2 DNA PURIFICATION

Purification of the linearized plasmids was carried out with the QIAquick ® Gel Extraction Kit (Qiagen, Germany). The DNA was combined with 5 volumes of PB buffer, further the sample was transferred to the column form the Kit. The first round of centrifugation was at carried out at 17.000xg for 1 minute at room temperature.

After this first centrifugation the columns were washed witch 750µl PE buffer. Another two rounds of centrifugation were performed.

For elution 30µl nuclease-free water (ThermoFisher Scientific, Germany) was incubated for 5min on the column and then finally centrifuged.

DNA concentrations were determined via Nanodop 1000 spectrophotometer (ThermoFisher Scientific, Germany)

3.3 DNA AGAROSE GEL ELECTROPHORESIS

For all DNA loaded gels 1g ultrapure agarose (Serva Electrophoresis GmbH, Germany) was dissolved in 100ml TAE buffer 1X (1% agarose gel). Agarose melting was performed in a microwave. Before pouring the gel, 4µl of 10mg/ml ethidium bromide (Roth, Germany) was added to the solution.

For a proper evaluation a size marker: 2-log DNA-ladder (NEB, Germany) was run along with the samples. The voltage used was in the range of 140 and 120 V for 20-30min.

5µl of each sample was combined with 2µl of 10x orange loading-dye (Carl Roth, Karlsruhe, Germany) and filled up with ultra-purified H2O (Biochrom AG, Germany) to 12µl total. Optical analysis was performed with FUSION Fx Vilber Lourmat device (Peqlab, Germany).

3.4 IN VITRO MRNA PRODUCTION

To avoid RNA degradation, it is highly necessary to remove all RNAse molecules from the surface of all instruments used. Therefor mRNA production of the two Talen was performed in a special dedicated RNA-hood which was, together with all instruments (e.g. pipettes), carefully cleaned with RNAse Zap (Sigma-Aldrich, Germany).

The protocol from the mMESSAGE mMACHINE® T7 Ultra kit (ThermoFisher Scientific, Germany) was followed for the transcription and also for the in vitro poly-A tailing reaction.

The procedure started with mixing 10µl T7 2x NTP/ARCA, 2µl 10x T7 reaction buffer and 2µl T7 RNA polymerase together with 1µg of purified linearized DNA to a total volume of 20µl. Incubation was performed at 37°C for 2 h.

After the transcription reaction, the DNA template was digested with 1µl TURBO DNase at 37°C for 15min. The tailing reaction was carried out by mixing 20µl 5X E-PAP buffer, 10µl MnCl2,

10µl ATP solution, 36µl nuclease-free water and 2µl E-PAP. After an incubation time of 40min at 37°C, the samples were placed on ice.

A recovery step by adding 50µl 7.5 M lithium chloride, 50mM EDTA was performed at -20°C for 30min. After centrifugation at 17.000xg at 4°C for 15min, the supernatant was removed and the RNA pellet was washed with 1ml 70% ethanol (Sigma-Aldrich, Germany). The centrifugation steps were repeated until all ethanol was removed by pipetting.

Finally the mRNA was resuspended in 11µl of RNAse free water (ThermoFisher Scientific, Germany). All aliquots were stored at -80°C.

RNA concentrations were determined via Nanodop 1000 spectrophotometer (ThermoFisher Scientific, Germany).

3.5 RNA GEL ELECTROPHORESIS

For evaluation of the RNA production, the mRNA was loaded on a denaturing formalehyde gel. The tailed RNA is expected to be relatively shifted in size compared with the simply transcribed form.

Before setting up the gel all surfaces and gel chambers were carefully cleaned with RNAse Zap (Sigma-Aldrich, Germany) and DEPC water (see 3.22). For the RNA-gel, 1g of agarose Serva for DNA electrophoresis (Serva GmbH, Germany) was melted in 75ml DEPEC water while heated in the microwave. As soon as all agarose had been dissolved, the solution was cooled to 60 °C and 10ml 10x MOPS (ThermoFisher Scientific, Germany) together with 18ml formaldehyde (Sigma Aldrich, Germany) were added. The whole solution was poured under a fume hood gently mixed into the tray where it polymerized.

For experimental control 500ng of polyadenylated mRNA was incubated with 8µl RNA loading-dye (NEB, Germany) and 1µl 200 µg/ml ethidium-bromide at 70°C for 5min. The same procedure was applied to 2µl of the mRNA sample before tailing. As sizemarker ssRNA ladder (NEB, Germany) was carried along next to the samples.

The loaded gel was run for 30min in 1x MOPS buffer.

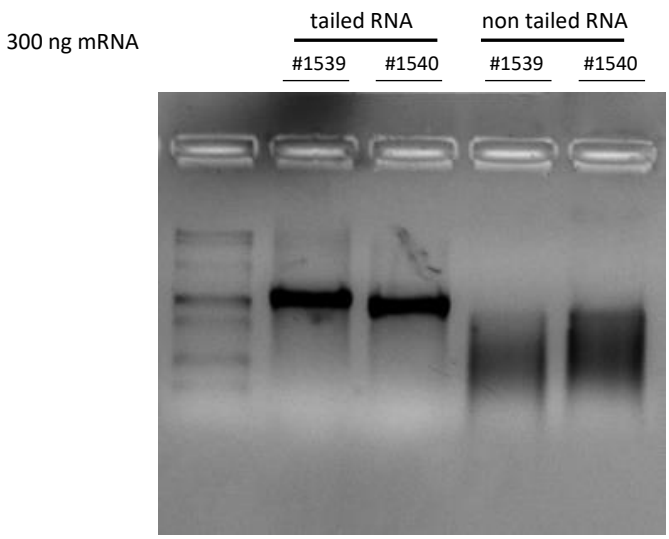

Figure 7: Example of a RNA agarose electrophoresis. 300ng mRNA were loaded either after PolyA-tailing (tailed RNA) or before (non-tailed RNA). The mRNA of the TALEN left subunit as well as the right subunit are shown (#1539/ #1540).

3.6 GENOMIC DNA EXTRACTION

QIAmp® DNA blood mini kit, (Qiagen, Germany) was used for gDNA extraction of the cultivated cells. The cells were either frozen as a pellet or used fresh for the extraction. The minimum amout of cells for this method was one confluent well of a 96-well plate (Sarstedt, Germany) while the maximum a cell number was $5x10^6$ cells.

The pellet was resuspended in 200µl PBS (PAN Biotech, Germany) and lysed with 4µl RNAse, 200µl buffer AL and 20µl Protese (Qiagen, Germany) were added ant incubated at 56°C for 10min.

After lysis, 200µl ethanol (Sigma-Aldrich, Germany) were added. The sample was transferred in a column and centrifuged at 6200xg for 1min. The filtrate was collected in a clean 2ml collection tube (Qiagen, Germany) which was replaced after each centrifugation.

After centrifugation, the column was washed with 500µl buffer AW1 and centrifuged again at 6200xg for 1min, 700µl washing buffer AW2 was used and the centrifugation was performed at maximum speed for 3min. In order to remove all residual ethanol, centrifugation at maximum speed was repeated for one more minute.

Elution of the DNA was carried out with 30µl ultra purified water (Biochrom AG, Germany). Before spinning at 6200xg for 1min, the column was incubated with the water for 5min to increase yield.

DNA concentrations were determined via Nanodop 1000 spectrophotometer (Thermo Fisher Scientific, Germany).

3.7 DIRECT CELL LYSIS OF LOW COUNT CELL SAMPLES

When the amount of cells did not reach a confluent 96 well, another protocol for gDNA extraction was chosen.

The cell pellet was mixed with 0,4µl 20mg/ml Proteinase K (Peqlab, Germany) and 19.6µl DirectPCR Lysis reagent (Peqlab, Germany), transferred to a PCR tube, vortexed and spinned down. Incubation was carried out in a thermocycler (Biometra, Germany) at 56°C for 1 h. and 45min at 85°C min to inactivate Proteinase K. After centrifugation, the supernatant was carefully harvested and transferred to a fresh Eppendorf tube.

3.8 POLYMERASE CHAIN REACTION

For amplification of the CCR5 locus and successful testing of genomic knockout - a special kind of PCR was used. In this “Touchdown” PCR the initial annealing temperature was higher than actual temperature required for the primers. With each cycle, the annealing temperature dropped by 1°C until the specific temperature for the primers was reached. Melting temperature is kept the same for all cycles. By following this PCR protocol the amplification of unwanted side products was decreased dramatically (50) (Table 4).

For the PCRs, Phusion HF polymerase (NEB, Germany), 5xPhusion HF Buffer (NEB, Germany) and dNTPs (NEB, Germany) were used (see Table 3). The primers were ordered from Apara Bioscience (Freiburg, Germany) (see Table 2).

	Primer ID	Sequence 5’ → 3’
TALEN 1	#1809	CAGTAGCTCTAACAGGTTGGACC
TALEN 2	#1820	CACTATGCTGCCGCCC

Table 2: PCR Primer for Touchdown PCR (33).

Substance	Amount per reaction
Primer #1809 (10µM)	0,8µl
Primer #1820 (10µM)	0,8µl
dNTPS 8 (40mM)	1µl
5X Phusion HF Buffer	10µl
Phusion (2000 u/ml)	0,35µl
gDNA	100ng
H_2O	Xµl
∑	50µl

Table 3: Ingredients of Touchdown PCR (33).

Step	Temperature	Time	Go To	Loops	ΔT
1	98°C	180s			
2	98°C	10s			
3	72°C	30s			-1°C
4	72°C	13s	2	5	
5	98°C	10s			
6	66,6°C	30s			
7	72°C	13s	5	33	
8	72°C	420s			
9	10°C	hold			

Table 4: Program of Touchdown PCR (33).

3.9 T7 ENDONUCLEASE 1 ASSAY

The T7 Assay was used to evaluate the genomic knockout of CCR5 by TALEN. The principle of this sensitive method is based on the particular properties of the T7E1 endonuclease. This enzyme recognizes single strand loops that form because of mismatches while denaturing and reannealing of the cleaved DNA fragments (see Figure 8) (51). InDel frequencies can be detected in the range of 5 to 95%. The cleavage by the T7 endonuclease is monitored on a 2% agarose gel. As positive control for this Assay HEK293T gDNA is used. This cell line has two CCR5 wildtype copies and one copy of the CCR5Δ32 locus.

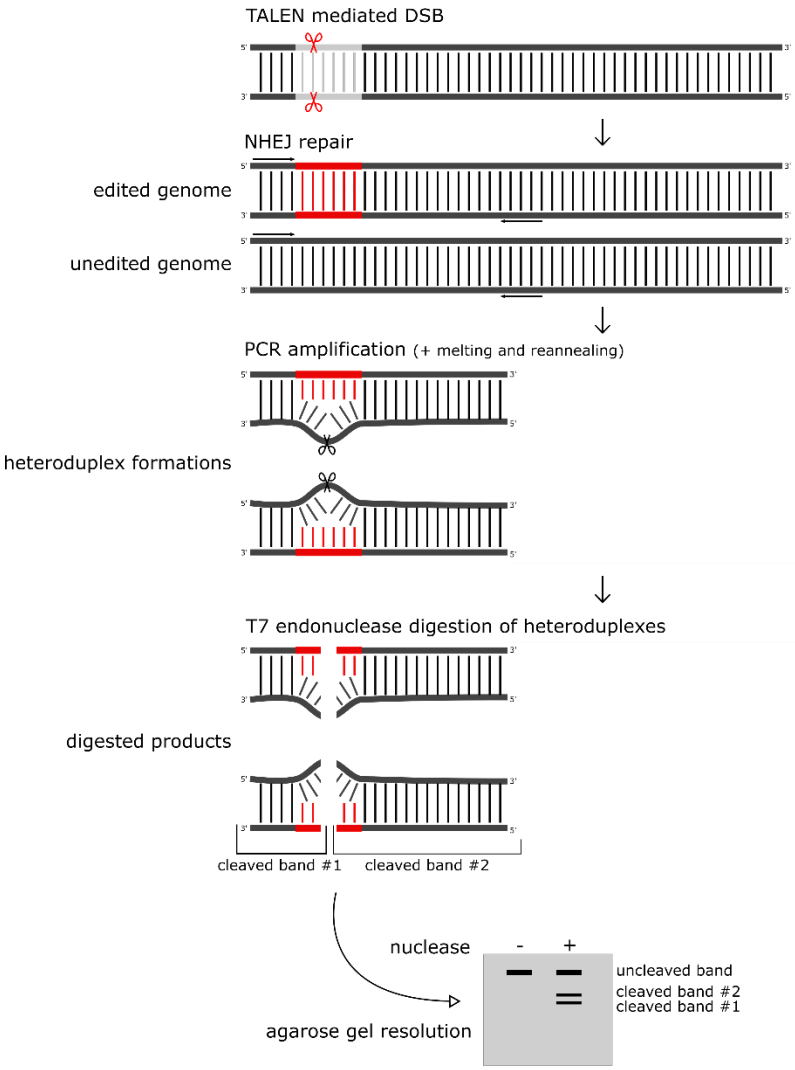

Figure 8: Scheme of T7 Endonuclease 1 assay. The DSBs which are induced by TALEN are repaired via NHEJ. The target locus is amplified by PCR, the amplicon is then melted and reannealed. When a wildtype and an edited strand reanneal a heteroduplex is formed. This heteroduplex formation is recognized and cleaved by the T7 enzyme. The successful cleavage can be monitored on a 2% agarose gel.

In the first step 25µl of purified PCR product are denatured in 3µl 10x NEB2 buffer (NEB, Germany) at 95°C for 5min. The following reannealing is performed by turning off the heating block. The samples cool down slowly to room temperature. After 3 h the actual T7 reaction can be started. For this, 200 ng of DNA are filled up to 13.5µl with 1x NEB2 buffer (NEB, Germany). Together with 0.75µl of T7endonuclease the reaction is digested for 20min in a 37°C water bath. The digestion is stopped by adding 3µl 10x orange dye (Carl Roth, Karlsruhe, Germany) and placed on ice. The result is evaluated on a 2% agarose gel which is run for 30min at 130 V.

3.10 T7E1-ASSAY EVALUATION

The 2% agarose gel was captured with a FUSION Fx Vilber Lourmat device (Peqlab, Germany). A .jpeg file was exported and analyzed with ImageJ (NIH). ImageJ was used to perform a digital quantification of the uncleaved band, cleaved band#1 and cleaved band #2 (see Figure 8). With the following formula the percentage of cleavage was calculated:

$$\%\ of\ cleavage = \frac{\text{"cleaved band\#1"} + \text{"cleaved band\#2"}}{(\text{"unleaved band"} + \text{"cleaved band\#1"} + \text{"cleaved band\#2"})} * 100$$

3.11 CD34$^+$ PREACTIVATION BEFORE NUCLEOFECTION

Two days before the nucleofection was carried out, CD34$^+$ cells were thawed and cultivated. The desired number of stem cells was thawed at 37°C in a water bath until barely any ice was visible. The cyrotube was slightly shaken by hand in the water bath. The cells were transferred into a 15ml tube (Greiner Bio One, Austria) in which they were carefully mixed by adding dropwise 1ml of prewarmed X-vivo 15 Media (Lonza, Switzerland). In order to mix the fluids the tube was gently flicked with a finger. Finally the tube was filled up to 15ml with warmed medium. The cells were now centrifuged at 300xg for 5min.

After removing the whole supernatant the remaining cell pellet was suspended in X Vivo 15 plus supplements. The amount of final medium was chosen according to a final concentration of 500,000 cells per ml (the cells were counted as described in chapter Cell counting3.18). 250,000 cells/well were transferred to a non-adherent 24-well-plate (Sarstedt, Germany) and incubated at 37°C.

3.12 NUCLEOFECTION

The transfer of mRNA into the cells was performed with a 4D-NucleofectorTM (Lonza, Switzerland). After counting the cells (see 3.18) the 100,000 cells/samples was pelleted (300xg for 5min) and the supernatant was discarded. The nucleofection medium was prepared using the P3 Primary Cell Nucleofector™ Kit (Lonza, Switzerland) by mixing 3.6µl of "Supplement" solution and 16.4µl "Nucleofector™ Solution" per sample. The cells were resuspended in 20µl of the nucleofection mix, transferred to a 20µl Nucleocuevette™ and then either 6µg of TALEN (3µg left TALEN + 3µg right TALEN) mRNA or 2µg of green fluorescence protein (GFP) mRNA were added to the mix. GFP mRNA was used to monitor transfer efficiency. The program used was DZ-100.

Directly after the nucleofection the samples were transferred to a non-adherent 96-well plate (Sartstedt, Germany) which already containeded 80µl of prewarmed medium. The medium was chosen accordingly to the cell type to be cultivated: cultivation of T cells, monocytes or $CD34^+$ cells. The samples were nucleofected one by one in order to minimize the time period of potential degeneration of the mRNA.

The 96-well plates were kept 24h at 32°C and 5% CO_2. This transient cold shock is known to increase the cleavage activity of TALEN. Originally Doyon et. al showed this fact with Zinc-Finger-Nucleases (ZNF) in slightly different conditions. However Emily Meyer who had been in AG Cornu before me, had already proven that the concept is valid for TALEN and the setup described above, too (52) (33).

All untreated samples were neither in contact with nucleofection solution nor did they receive a pulse like the treated ones. One day after nucleofection the cells expressing GFP could be analysed via flow cytometry and the efficiency of the experiment could then be determined.

3.13 MAINTENANCE OF OP9-DL1

OP9-DL1 cells were kept on α-Minimum essential medium (α-MEM). 5g of α-MEM powder (Gibco Life Technologies, USA) were dissolved in 485.4ml ultra-purified H_2O (Biochrom AG, Berlin, Germany) and 14,6ml 7.5% sodium bicarbonate (Gibco Life Technologies, USA) were added. The solution was filtered through a 0.22µm bottle top filter (Corning, USA). Storage time for this stock solution was max. 2-3 weeks at 4 °C.

To complete the medium 195ml of the stock solution were combined with 50ml HyClone Defined Fetal Bovine Serum (FBS) OP9-FCS (GE Healthcare Ltd, UK) to a final concentration of 20% as well as with 2.5ml P/S (Sigma-Aldrich, USA) and 2.5ml L-Glutamine (GE Healthcare Ltd., UK.).

Cultivation: for the T cell differentiation OP9-DL1 cells were used as feeder cells. OP9-DL1 were cultivated in a T-75 flask (Sarstedt, Germany) at 37 °C in an incubator (Heracell 240i, Thermo Fisher Scientific, Waltham, MA, USA) with 5% CO_2 and splitted every 3 days.

To split the cells, the medium was removed, the cells were washed with 10ml PBS buffer (PAN Biotech, Germany) and then incubated with 1.5ml Trypsin-EDTA (10x) (Germany) at 37 °C for 5min. After detaching, 8.5ml of complete medium was added to the cells, the cells were collected and centrifuged at 2336xg for 5min. The supernatant was removed and the cells were resuspended in 1ml of complete medium in order to count the cells.

The cells were then seeded at a density of 250,000 cells in 15ml complete medium and transferred to a T75–flask (Sarstedt, Germany).

Two days before starting the T cell differentiation, a 6-well plate per sample with 50,000 OP9-DL1 cells in 1ml complete medium was prepared. Alternatively, one day before differentiation 100,000 OP9-DL1 cells could be seeded as well.

3.14 CULTIVATION OF $CD34^+$ CELLS

The freshly thawed $CD34^+$ cells were counted with NucleoCounter (ChemoMetec, Denmark). For cell number and viability analysis the cells were stained with Solution 18 (ChemoMetec, Denmark).

$CD34^+$ cells were cultivated in X-Vivo 15 (Lonza, Switzerland) without antibiotics. Due to this fact the medium was filtered through a 0.22µm filter (Merck Millipore Ltd., Germany) as an extra precaution to avoid any contaminations after supplementing with the cytokine cocktail. As supplements 25ng/ml rhSCF (ImmunoTools, Germany), 50ng/ml rhTPO (ImmunoTools, Germany), and 50ng/ml rhFLT3 (ImmunoTools, Germany) were added to the medium.

Whenever $CD34^+$ cells were not used for any nucleofections, 20ng/ml IL-3 (ImmunoTools, Germany) and 20ng/ml IL-6 (ImmunoTools, Germany) were supplemented in order to boost proliferation.

3.15 DIFFERENTIATION OF $CD34^+$ CELLS TO MONOCYTES

100,000 $CD34^+$ cells were transferred to a 24-well plate (Sarstedt, Germany) in 500µl of three different differentiation media. 500µl α-MEM (protocol 3.13) for each well was supplemented with 50ng/ml M-CSF (Immunotools, Germany) or 25ng/ml IL-3 (Immunotools, Germany) or both in combination. The cells were kept in the adherent 24-well plate till the wells were confluent, which could last up to 10 days, depending on the donor and also the medium selected. Then, the cells were transferred to an adherent 6-well plate (Sarstedt, Germany) where 1ml of each differentiation media was added.

At every harvesting the medium was completely exchanged. Fresh medium was added whenever the pH-indicator strongly changed colour. The medium and cells were visually checked every second day.

Splitting and harvesting: the cells were transferred to a 50ml falcon (Greiner Bio one, Austria). Afterwards the wells were washed with 1ml PBS buffer (PAN Biotech, Germany). The cells that remained on the bottom of the well were harvested using a cell scraper S (TPP, Switzerland). Scraping was performed in 800µl PBS. The scraper and the well were rinsed with 1ml PBS. The well was then first rinsed with 5ml PBS and afterwards one more time with 10ml PBS.

The whole falcon was centrifuged 7min at 300xg at 14 °C. After removing the whole supernatant, the cells were resuspended in 1ml complete medium and then counted as described below. After taking the required number of cells for flow-cytometry analysis the rest of the cells were reseeded preferentially with a density of 50,000 in a 24-well plate.

3.16 DIFFERENTIATION OF $CD34^+$ CELLS TO T CELLS

T cells were co-cultured with OP9-DL1 cells. On adherent 6-well plates (Sarstedt, Germany) OP9-DL1 cells were seeded 1-2 days before transferring $CD34^+$ cells, as described above. Addition of 300,000 CD34 cells on the already colonized dish was carried out dropwise and very carefully to not disturb the layer of feeder cells.

In the first week 1ng/ml rh-IL7 (Immunotools, Germany), 2ng/ml rh-SCF (Immunotools, Germany) and 2ng/ml rh-Flt3 (Immunotools, Germany) were added to the complete α-MEM-media. From the second week onwards, rh-SCF and rh-Flt3 were removed.

The volume was kept at 2ml total and fresh medium was added every week at the harvesting and flow cytometry analysis time-points. After the flow cytometry analysis the following cytokine cocktail was used: If CD7 expression was extremely high, IL-7 was removed (10^5 fluorescence units in the flow cytometry analysis). For high CD7 expression IL-7 was reduced to 0,5ng/ml (10^4-10^5) and for low CD7 (max. 10^4) IL-7 was kept at to 1ng/ml. As soon as CD4/CD8 double positive cells are detected, 2ng/ml IL-2 should be supplemented to increase the amount of this population.

3.17 HARVESTING OF T CELLS

All cells were filtered through a 70µm cell strainer (BD, USA) into a 50ml falcon (Greiner Bio-one, Austria). This filtration was performed to remove OP9-DL1 and increase the ratio of T cells to feeder cells for the flow-cytometry analysis. When all liquid was transferred to the filter/falcon the well was gently washed with 1ml PBS (PAN Biotech, Germany) without disrupting the layer of adherent cells, in order to remove all T cells lying loosely on the feeder cells. With another 1ml PBS the layer was destroyed and completely resuspended until no cell-clumps were visible any more. Additionally, 5ml were used to transfer the rest of the cells to the falcon. Finally, the well was rinsed with 10ml PBS. Before centrifugation the filter was squeezed -without damaging it – to press out the remaining drops. Then the sample was centrifuged 7min at 300 x g at 14 °C. After removing the supernatant, the cells were resuspended in 1ml of medium supplemented with 2ng/ml rhIL-7 and then counted (see 3.18). Finally after the analysis, the T-cells were reseeded to a well containing 1ml complete α-MEM-media and OP9-DL1 feeder cells.

3.18 CELL COUNTING

OP9-DL1 cells, T cells and monocytes were counted visually with a Neubauer improved counting chamber (Marienfeld, Germany). Trypan blue solution (Sigma-Aldrich, USA) was used to distinguish living cells from dead cells. The following formula was used to calculate the actual cell number:

$$cell\ number = \frac{x(counted\ cells) * d(dilution\ factor) * v(volume) * 10^4}{4(squares)}$$

3.19 ANTIBODY STAINING FOR FLOW CYTOMETRY ANALYSIS

For each time-point preferentially at least 50,000 monocytes / T cells or at least 10,000 $CD34^+$ cells were harvested and stained.

Only the monocytes samples were incubated 5min at room temperature with 1µl FC-block (BD Bioscience, USA) in 25µl flow-cytometry buffer previous to staining.

The cells were washed with 1ml of flow-cytometry analysis buffer, centrifuged 5min at 300 x g and the whole supernatants removed. The desired master-mix of antibodies was added and the samples were incubated in the fridge at 4 °C for 20min. Directly after staining the cells were washed again with 1ml flow-cytometry analysis buffer and then centrifuged. 1µl DAPI (Sigma-Aldrich, USA) in 1ml flow-cytometry buffer was used for this second washing step in some of the samples. After removing the supernatant the cells were resuspended in 270µl of flow-cytometry buffer and stored in the fridge or on ice till flow cytometry analysis.

The time between staining and measurement was always within max. 3 hours.

3.20 FLOW CYTOMETRY

All flow cytometry measurements were performed either with the BD FACS CANTO II (BD Biosciences, USA) or the BD Accuri C6 (BD Biosciences, USA) devices. The software used for capturing was “DIVA” and the analysis were done with “Flow Jo”.

The amount of counted events to be collected was 5,000.

mastermix for T cells staining			mastermix for monocyte staining		
antibody	fluorochrome	company	antibody	fluorochrome	company
CD1α	APC/Cy7	Biolegend	CD4	PE-Cy7	eBioscience
CD4	PE-Cy7	eBioscience	CD14	PE-Cy7	BD Biosciences
CD5	FITC	Macs Miltenyi	CD45	FITC	Biolegend
CD7	PerCP-CP5.5	BD Biosciences	CD33	PerCP-Cy5.5	Biolegend
CD8	AmCyan	BD Biosciences	CCR5	APC	BD Biosciences
CD34	PE	BD Biosciences			
CCR5	APC	BD Biosciences			

Table 5: List of antibodies used in the two different cell stainings

3.21 FLOW CYTOMETRY ANALYSIS BUFFER

Flow cytometry analysis-PBS (PAN Biotech, Germany) enriched with 0,1% 100 mg Sodium Azide (Sigma-Aldrich, Germany) and 1 mM EDTA (Sigma-Aldrich, Germany).

3.22 DEPC WATER

To clean the instruments used for RNA production, ddH_2O is mixed with 1ml/l DEPEC (Sigma-Aldrich, Germany). After 1 hour of swirling, the water is autoclaved.

3.23 10X MOPS

To obtain a 10x solution, 41.8 g MOPS (Thermo Fisher Scientific, Germany) was dissolved in 400ml DEPC water. After the pH was adjusted to 7,0 using 1M NaOH, up to DEPC water was filled up to 700ml, 20ml DNAse- and RNAse-free 0,5 M EDTA (Promega, USA) together with 20ml 1M sodium acetate (Thermo Fisher Scientific, Germany) were added as well. The final volume was adjusted to 1 l was by filling up with DEPC water. Subsequently the solution trough a 0,45µm millipore filter. The complete 10x MOPS solution was wrapped in aluminium foil in order to keep protect from light and was kept at 4° in the fridge.

3.24 50X TAE BUFFER

242mg 80mM Tris base (AppliChem, Germany), 57,1ml 0,1% acetic acid (Sigma-Aldrich, Germany) and 100ml of 0,5M ethylendiaminetetraacetic acid (EDTA) (Sigma-Aldrich, Germany) were added to 700ml ddH2O.

To remove undissolved salts a 0.45µm Millipore filter was used and finally the pH was adjusted to 8.5 using dd H_2O.

3.25 6X ORANGE DYE

40mg Orange G (Carl Roth, Karlsruhe, Germany), 3ml glycerol (Merck, Darmstadt, Germany) and a variable volume of ddH2O (Biochrom AG, Berlin, Germany) were mixed up to a final volume of 10ml.

RESULTS

4.1 CORD BLOOD EVALUATION

As starting material $CD34^+$ cells derived from cord blood were isolated. The cord blood was kindly provided by the Frauenklinik of Freiburg after informed consent and ethics committee approval. Cell separation was performed by Ilona Skatulla, a technician of AG Cornu. After isolating the $CD34^+$ cells, they were frozen and stored in liquid nitrogen.

Before the stem cells could be seeded for either T cell differentiation or monocyte differentiation, a recovery period of 2 days in culture medium had to be carried out. The cells were evaluated via flow cytometry on day 0 (thawing) and day 2 (seeding for differentiation). Three different parameters were tested: CD34, CD38 and CCR5. CD34 and CD38 are known to be typical markers of HSCs in cord blood (53). They are characteristic for this cell subset and can be therefore used to validate the starting material and the cells' differentiation potency, too. As one aim has been to track CCR5 during the whole process of differentiation, the starting material had to be checked as well. $CD34^+$ cells never showed any significant levels of CCR5 during the experiments. As there were no significant differences regarding surface markers, respectively CD34/CD38, (data not shown) in between these two time-points, day 2 was chosen for later evaluations.

Figure 9 (A) shows the applied gating strategy. 91.5% of all events were clustered in a compact population (one experiment exemplarily shown). This population corresponds to the desired population. A viability staining with DAPI was performed to exclude dead cells and debris. To determine the "stemness" of the cells, CD34 and CD38 were monitored. These markers are characteristic for stem cells in early stages CD34+/CD38- cells are correspond to a very primitive subpopulation of CD34 cells. CD34 is lost early in the course of differentiation and therefore indicates an early progenitor in combination with a good stemness. As expected, hardly any CCR5 co-receptor (1.76%) could be detected on the stem cells.

99.7% (includes ± error bars values) of the cells which were seeded later had been positive for CD34. Additionally 79.5% (includes ± error bars values) of all acquired cells had been both CD34 and CD38 double positive. Figure 9 (A) shows an exceptional donor with only 2% $CD34^+/CD38^-$ cells. The numbers above represent the average of 3 independent experiments (Figure 9 (B)).

A

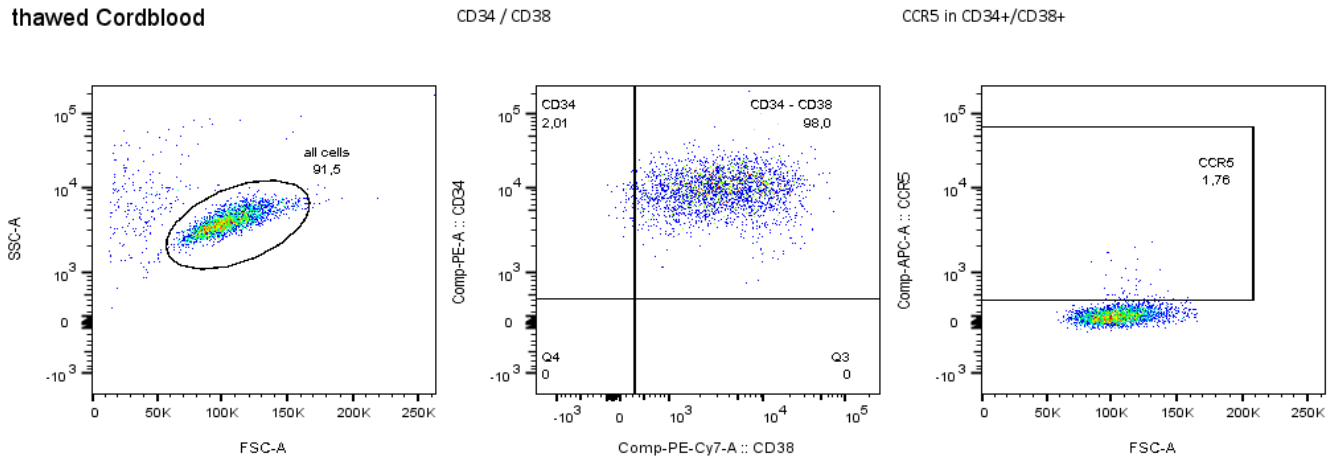

B

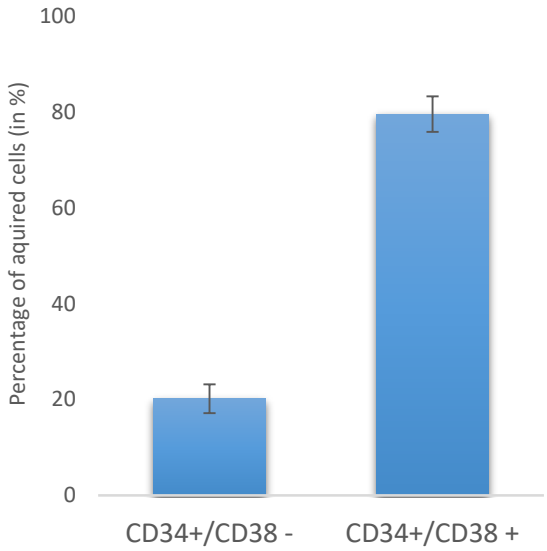

Figure 9: Flow cytometry analysis of cord blood at day 2 after thawing. (A) The gate was set on the FSC and SSC parameters, CD34 and CD38 were detected in these cells. Panel 3 shows the amount of CCR5 on the surface of CD34+/CD38+ double positive cells. (B) The median of CD34+/CD38- and CD34+/CD38+ over three experiments is displayed.

4.2 T CELL DIFFERENTIATION

The differentiation of T cells was performed over a period of 4 weeks. In each week a staining with antibodies specific for several CD markers on the cells surface was carried out. The gating strategy for these stainings consisted of multiple gating strategy. As shown in (Figure 10 (B)) 5 stages of T cell development can be defined by their surface markers. Due to similar CD markers the stages of ISP and DP cells were fused into one stage: ISP/DP.

Early T-progenitor (ETP) cells were defined as CD7 negative and CD34 positive. This subset was negative for CD5 and CD1α, too. T cell progenitor (Pro-T) cells were in comparison to ETPs positive for CD 7 and positive for CD34. In contrast to all cells in earlier stages Pre-T represented the first subset which had already lost CD34 on its surface. CD1α and CD5 were both found on Pre-Ts, but on Pro-Ts only CD 5 could be detected. Finally, a subset without CD34, CD7, CD5 and CD1α was considered to represent immature single or immature double positive (ISP/DP) cells.

The four different stages were monitored by the following gating strategy: initially the T cell population was gated and excluded from feeder cells using FSC and SSC parameters (Figure 10 (A)). Within this population, the CD4/CD8 double negative cells were chosen, and subsequently analysed for the expression of CD34 and CD1a. This panel constitutes the basis for distinguishing different cell stages during the process of differentiation.

In the course of 4 weeks, the proportion of the different subsets changed. The progress of differentiation is shown in Figure 10 (C) (one experiment is exemplarily shown). In week 1 ETPs and Pro-Ts represent the majority of cells. The second staining in week 2 showed a strong decrease of ETPs as well as of Pro-Ts. However, the subset of Pre-Ts increased in week 2. From week 3 on almost no ETPs could be detected. Also Pro-Ts declined strongly and were finally absent in week 4. Pre-Ts could be monitored till week 4. The peak of Pre-Ts showed up in week 2 and from then on the numbers constantly decreased.

According to the theoretical considerations the cells performed a cycling: each of the four weeks of differentiation showed a unique pattern. Young cells close to stem cells, especially seen at the beginning of the experiment, decreased overtime as most of these cells aged and became more differentiated.

Not only the proportion of the different subsets changed over time, but the overall size of the whole population changed as well (Figure 10 (D)): the longer the differentiation process lasted, the smaller the cells became. This fact refers to the well described cell sizes of stem cells and T cells. T cells are known to be small cells with a diameter of 7-8 µm. In contrast to T cells, stem cells are larger (54). The reduction of cell size during the process of *in-vitro* differentiation emphasizes its similarity to the physiological differentiation *in-vivo:* The *in-vitro* differentiated cells show the same properties as *in-vivo* differentiated cells.

A

CB to T-cells

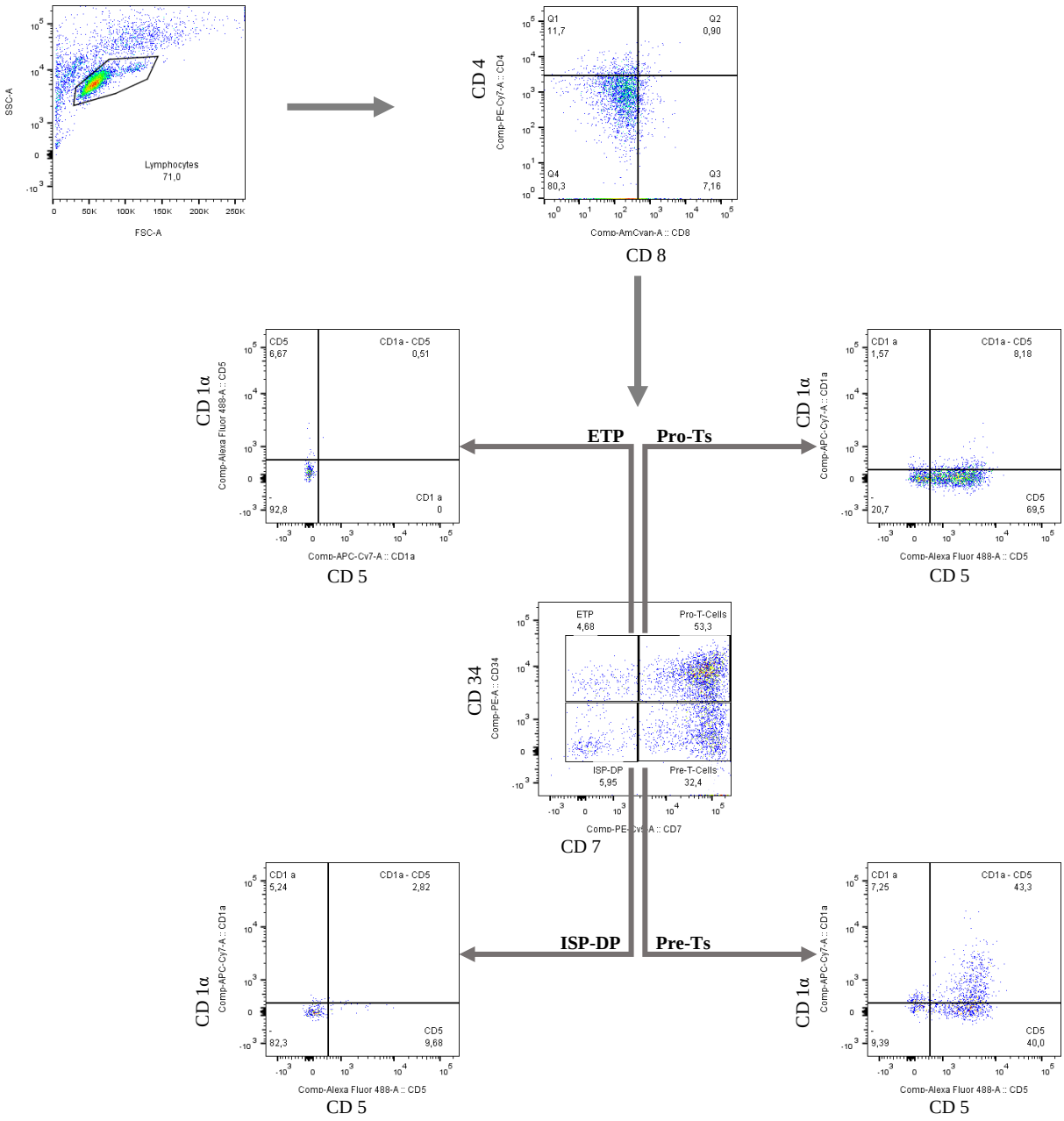

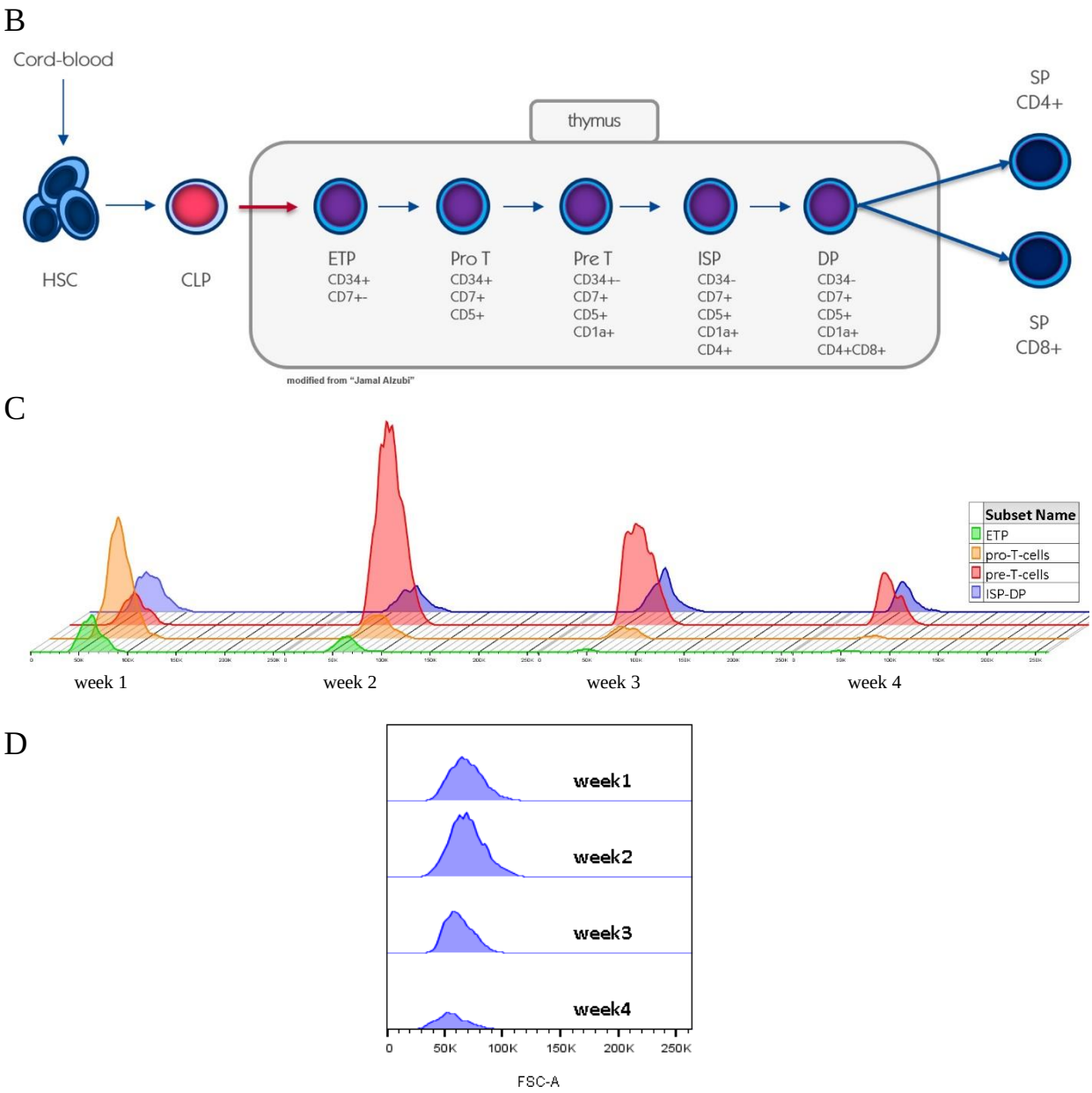

Figure 10: Schematic view on T cell differentiation and flow cytometry analysis of the T cell differentiation set up. Staining was performed weekly, the indicated surface markers where targeted via fluorescent antibodies. (A) Gating strategy, exemplary for week 2. OP9-mDL1 feeder cells were distinguished from all T cell progenitors by size in the first plot using the forward and side scatter. The CD4/CD8 double negative cells were selected and further monitored in terms of to CD34 and CD7. In this panel four different types of subsets could be found. These subsets were subsequently proven by their characteristic phenotype. CD1α and CD5 were negative in both early T-progenitors (ETP) (CD34+/CD7-/ CD5- /CD1α-) and immature single/double positive cells (ISP-DP). In T cell progenitors (pro-Ts) (CD34+/CD7+/ CD5+ /CD1α-) at least CD1 α and in T cell precursors (pre-Ts) (CD34-/low/ CD7+/ CD5+ /CD1α+) even both CD1α and CD5 were positive. (B) Overview of the four different stages of T cell precursors during physiological differentiation. Hematopoietic stem cells (HSC) differentiate into common lymphoid progenitors (CLP). In the thymus the cells reach further stages: early T-progenitors (ETP), T cell progenitors (Pro-Ts), T cell precursors (Pre-Ts) and immature single/double positive cells (ISP-DP). Finally they are exported from the thymus and become single positive cells (SP). (C) Subset analysis quantification and monitoring during 4 weeks of differentiation in (percentage of the whole population at each time point). In each week of measurement the different subsets changed. (D) Size of the lymphocyte subset of T cell cells during the measuring period.

4.3 CCR5 EXPRESSION DURING T CELL DIFFERENTIATION

In order to evaluate which T-cell precursors are already targets for HIV, CCR5 was tracked during expressed on these immature T-cells.

CCR5 expression was monitored in all 4 subsets described above during 4 weeks of differentiation. Figure 11 displays the quantification of the CCR5 expression on the subsets. In ETPs barely any CCR5 could be detected (5%) whereas in the Pro-T stage CCR5 was strongly expressed on the surface of the cells (21%). In both the Pre-T stage and the ISP-DP stage CCR5 surface expression could be detected to a similar extent: 29%.

As indicated by the error bars the amount of detected CCR5 varied strongly between the different experiments. Material from three different donors in three independent experiments was used. The earliest stage of differentiation at which CCR5 could be detected was in between the stages of pro-Ts and pre-Ts. Some donors' cells expressed CCR5 already at the pro-T stage and others not until pre-T stage.

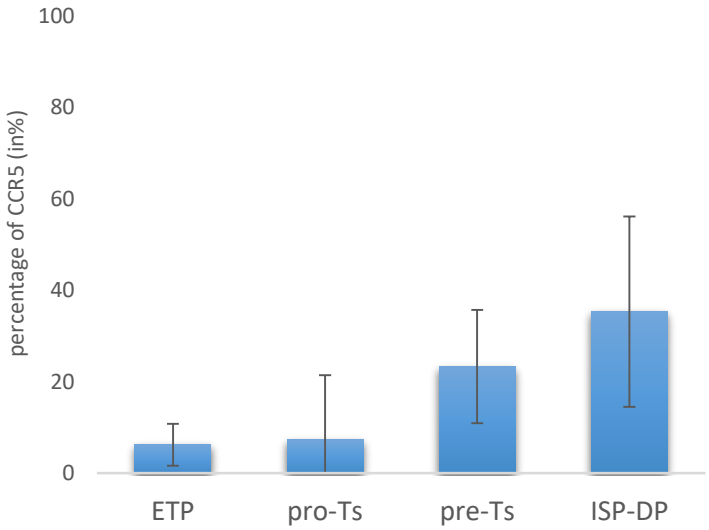

Figure 11: Statistical analysis of CCR5 expression in T cell progenitors measured by flow cytometry of three independent experiments. The bars display the median CCR5 in four subsets with data from all time-points during the period of differentiation (4 weeks).

4.4 MONOCYTE/MACROPHAGE DIFFERENTIATION

The differentiation of monocytes/macrophages was evaluated at two different time-points. In total 4 different cytokines cocktails were compared: IL-3 alone, M-CSF alone, a combination of both IL-3 plus M-CSF and a condition named "change". "Change" condition started with only M-CSF and after 5 days IL-3 was added to the cell culture. The first harvesting was carried out between day 10 and day 13. The second harvesting took place between days 16 to 19. In parallel to the T cell differentiation experiments the monocytes/macrophages were analysed via flow-cytometry.

The gating strategy started with removing the debris by gating the cells by their size, further dead cells were excluded by a viability staining with DAPI. All living cells were analysed for CD33 and CD14. In $CD33^+/CD14^-$ and $CD33^+/CD14^+$ cell populations both CCR5 and CD4 were monitored.

The phenotype of pre-monocytes is pinpointed in Figure 12 (B): monoblasts are only $CD45^+$, whereas pro-monocytes are $CD45^+$ as well as $CD33^+$. Almost mature monocytes can be found to be $CD33^+/CD14^+$ double positive. CD45 was not included in the antibody stainings because the focus laid on pro-monocytes and monocytes but not on monoblasts.

Figure 12 (A) shows exemplarily media condition IL-3 at the first harvesting time-point. $CD33^+$ single and $CD33^+/CD14^+$ double positive cells could be detected. In the double positive population CD4 and CCR5 were expressed on nearly half (48%) of the cells. The vast majority (77%) of all $CD33^+/CD14^+$ cells expressed CCR5. In contrast, barely any $CD33^+$ single positive cells showed CCR5 and CD4 on their surface.

Figure 12 (C) illustrates the comparison of the four different media conditions. Panel 1 shows the median of 3 independent experiments at the first time-point harvesting. IL-3 and IL-3+M-CSF in combination showed a similar distribution of CD33 single positive and CD33/CD14 double positive cells. Nevertheless, IL-3 in combination with M-CSF seemed to induce higher numbers of CD33/CD14 double positive cells than IL-3 alone (15.1% in IL-3 vs. 26.8% in IL-3+M-CSF (first time-point)). M-CSF had the greatest potential to achieve double positive cells (55.95% at first time-point; 58.35% at second time-point). As shown in Figure 12 (E) M-CSF impaired cell proliferation when compared to the other conditions. For this reason this condition was only carried out once and the "change" condition was established (which was also only evaluated once): In order to boost cell proliferation IL-3 was added to the "M-CSF only" condition after 5 days. This

condition could not generate the high percentage of double positive cells which has been observed in M-CSF alone (M-CSF: 1. Harvesting 56%, 2. Harvesting 58% vs. Change: 1. Harvesting 37%, 2. Harvesting 34%). Nevertheless, the percentage of double positive cells was higher than in samples with IL-3 alone (IL-3: 1. Harvesting 15%, 2. Harvesting 30%).

At the second harvesting time-point (Figure 12 (C)) a similar percentages of subsets for all media conditions could be found. The number of CD33/CD14 double positive cells was very similar in two media conditions except condition change. For IL-3 condition, the median of $CD33^{+}/CD14^{+}$ cells was 14.4% higher than in the first harvest, whereas it increased for M-CSF 2.4% and IL-3+ M-CSF 5.3%. Only in the condition change the median of double positive cells was 2.5% lower, but is not significant.

A difference in terms of size of the total cell population was also observed during differentiation. Figure 12 (D) displays the size of the basic population determined by FSC/SCC at the first and second harvesting. The most differentiated cells appeared to be bigger than the less differentiated ones. Especially in the media containing M-CSF alone the mean of cells size was about 40% bigger than with IL-3 alone. Condition “change” has not been analysed regarding cell size.

The total cell numbers were determined at the first harvesting time-point and shown in Figure 12 (E). The starting material had been 60,000 cells for each condition. The first panel of (E) shows the starting cells number and total cell number at the first harvesting time-point, while the second panel displays the replication-factors, which indicate how often the cells have replicated till the harvesting time-point. To determine these factors, the cell number at the first harvesting time-point was divided by the initial number of cells.

As M-CSF alone generated very low cell numbers in the first experiment, the media condition change was therefore established in the second experiment. The analysis of both media conditions do not include deviation graphs because both conditions have been tested only once. The data shown for the media conditions IL-3 and IL-3 + M-CSF includes two independent experiments.

The media conditions containing IL-3 showed in both experiments a good yield: the median was 962,500 cells. In the first experiment in which IL-3 + M-CSF was used the total number of cells was 1,625,000 and in the second experiment the number of cells was 800,000. The median for IL-

3 + M-CSF was then 1,212,500. The total amount of cells with a number of 85,000 for the media condition M-CSF was rather low. The media condition change generated 825,000 cells.

In conclusion all media conditions containing IL-3 provide an environment which supports cell proliferation. The direct comparison of IL-3 and IL-3+M-CSF shows a very similar potency to promote cell proliferation of both conditions. Possibly IL-3+M-CSF could even outperform IL-3 alone. Nevertheless more experiments need to be done in order to specify the difference between these media conditions statistically. The fact that M-CSF alone shows a very poor ability to support cell proliferation is very obvious. For this reason the condition “change” has been established. Adding IL-3 to cultures with M-CSF only creates a boost of cell proliferation even at later time points in cell culturing.

A

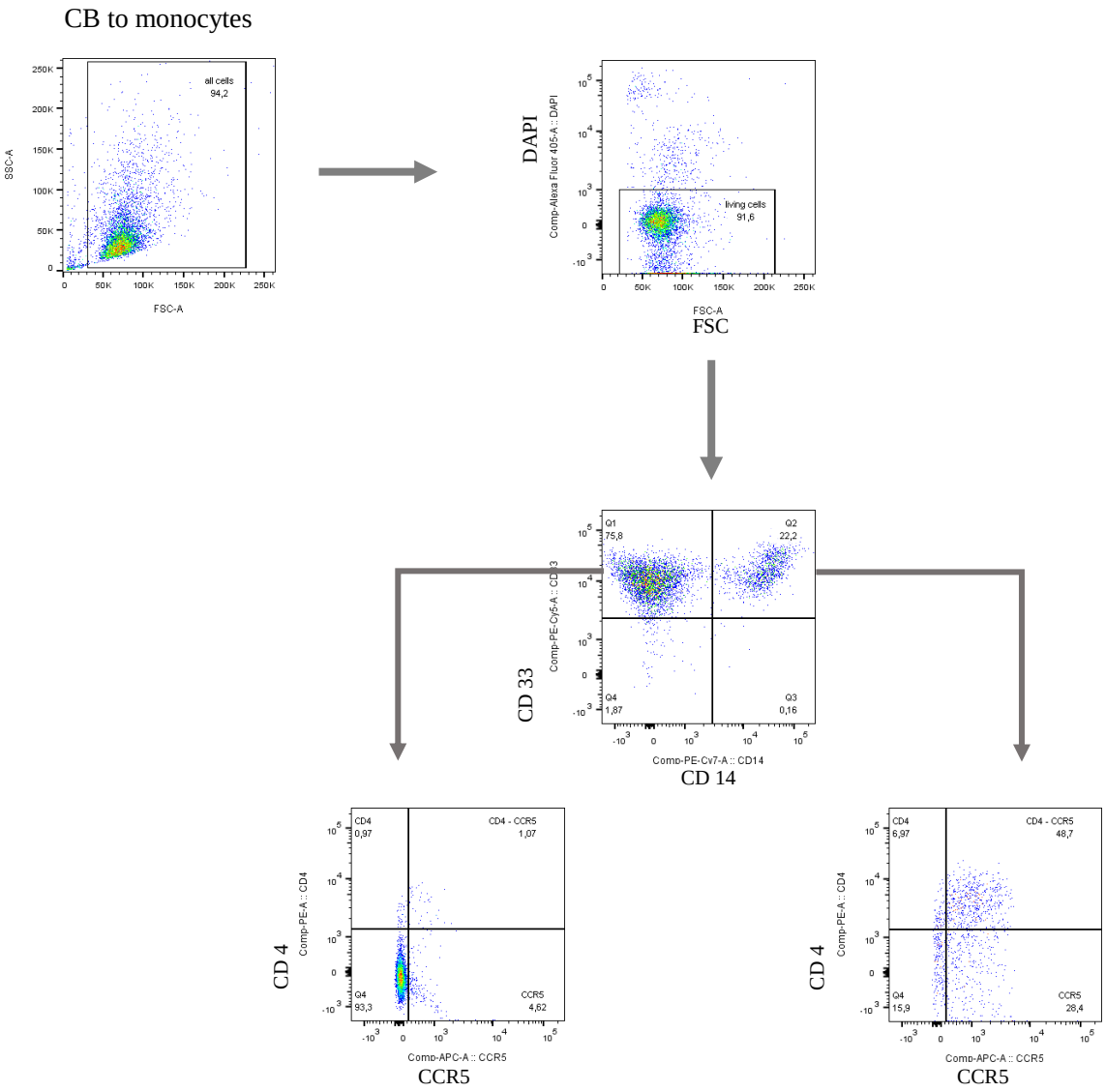
CB to monocytes
all cells
94,2
SSC-A
FSC-A
DAPI
living cells
91,6
FSC
CD 33
CD 14
Q1
75,8
Q2
22,2
Q4
1,87
Q3
0,16
CD4
0,97
CD4 - CCR5
1,07
Q4
93,3
CCR5
4,62
CD 4
CCR5
CD4
6,97
CD4 - CCR5
48,7
Q4
15,9
CCR5
28,4

B

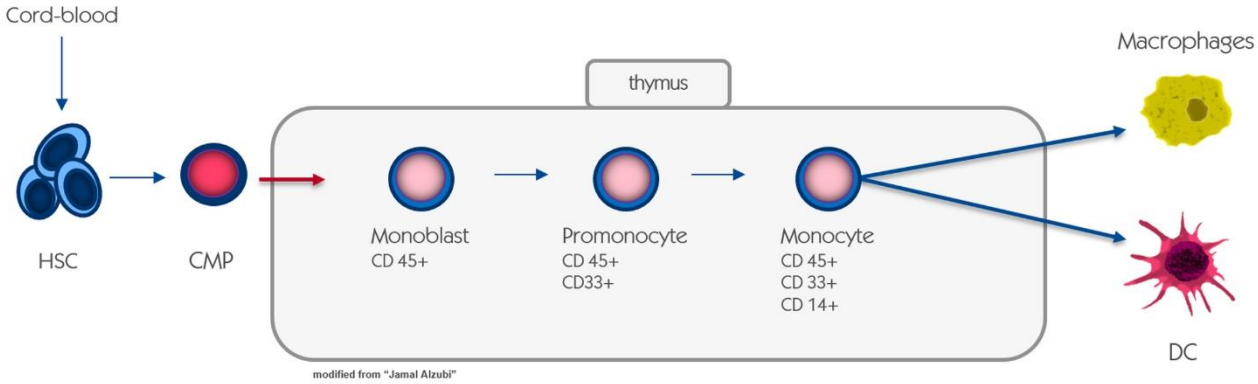
Cord-blood
HSC
CMP
thymus
Monoblast
CD 45+
Promonocyte
CD 45+
CD33+
Monocyte
CD 45+
CD 33+
CD 14+
Macrophages
DC
modified from "Jamal Alzubi"

C

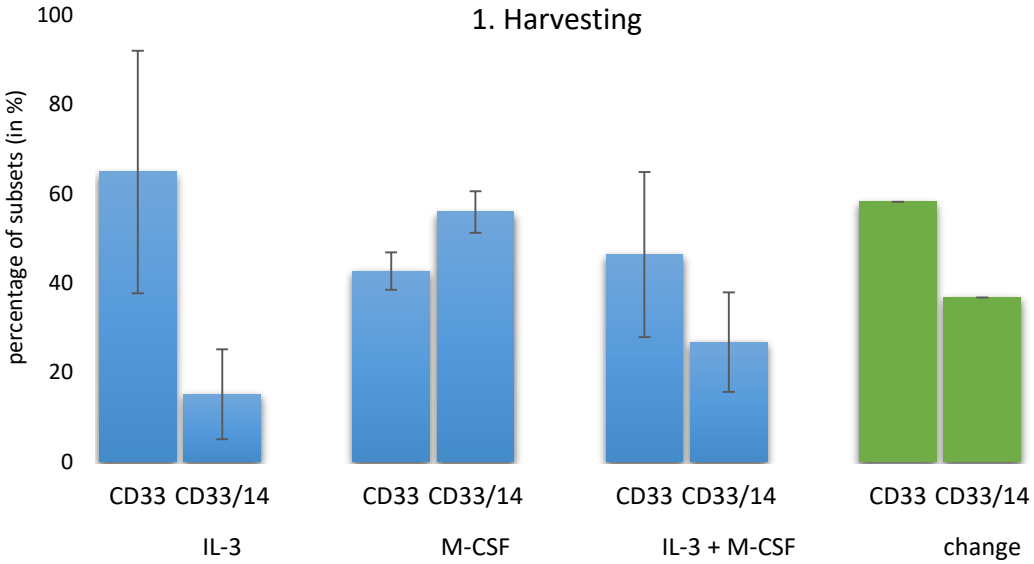
1. Harvesting
percentage of subsets (in %)
100
80
60
40
20
0
CD33 CD33/14
IL-3
M-CSF
IL-3 + M-CSF
change

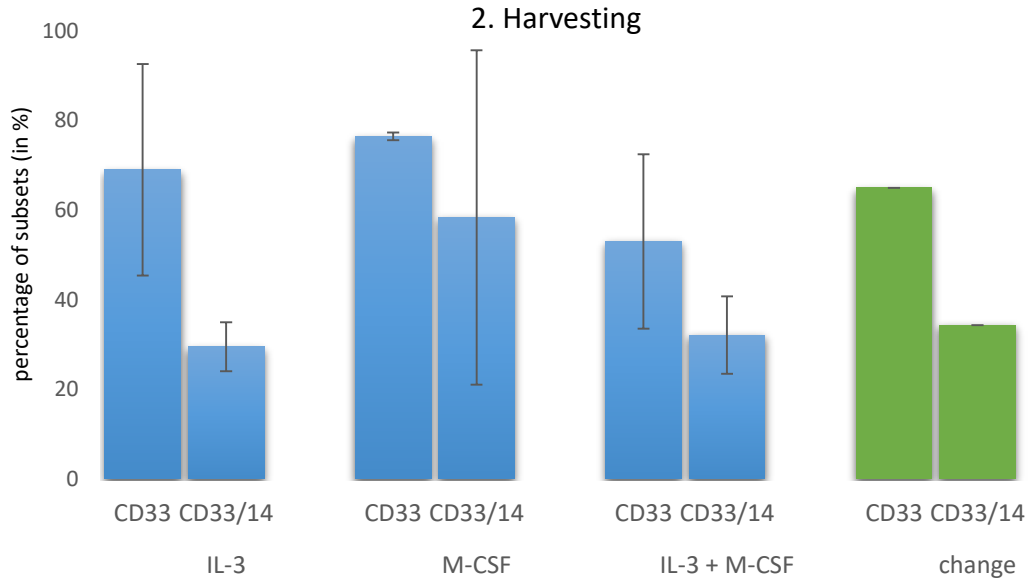
2. Harvesting
percentage of subsets (in %)
100
80
60
40
20
0
CD33 CD33/14
IL-3
M-CSF
IL-3 + M-CSF
change

D

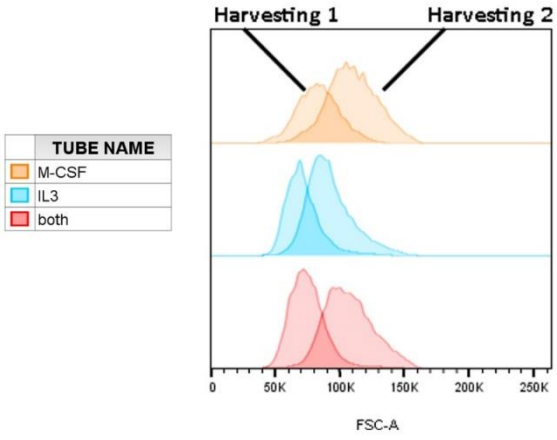
Harvesting 1
Harvesting 2
TUBE NAME
M-CSF
IL3
both
0
50K
100K
150K
200K
250K
FSC-A

E

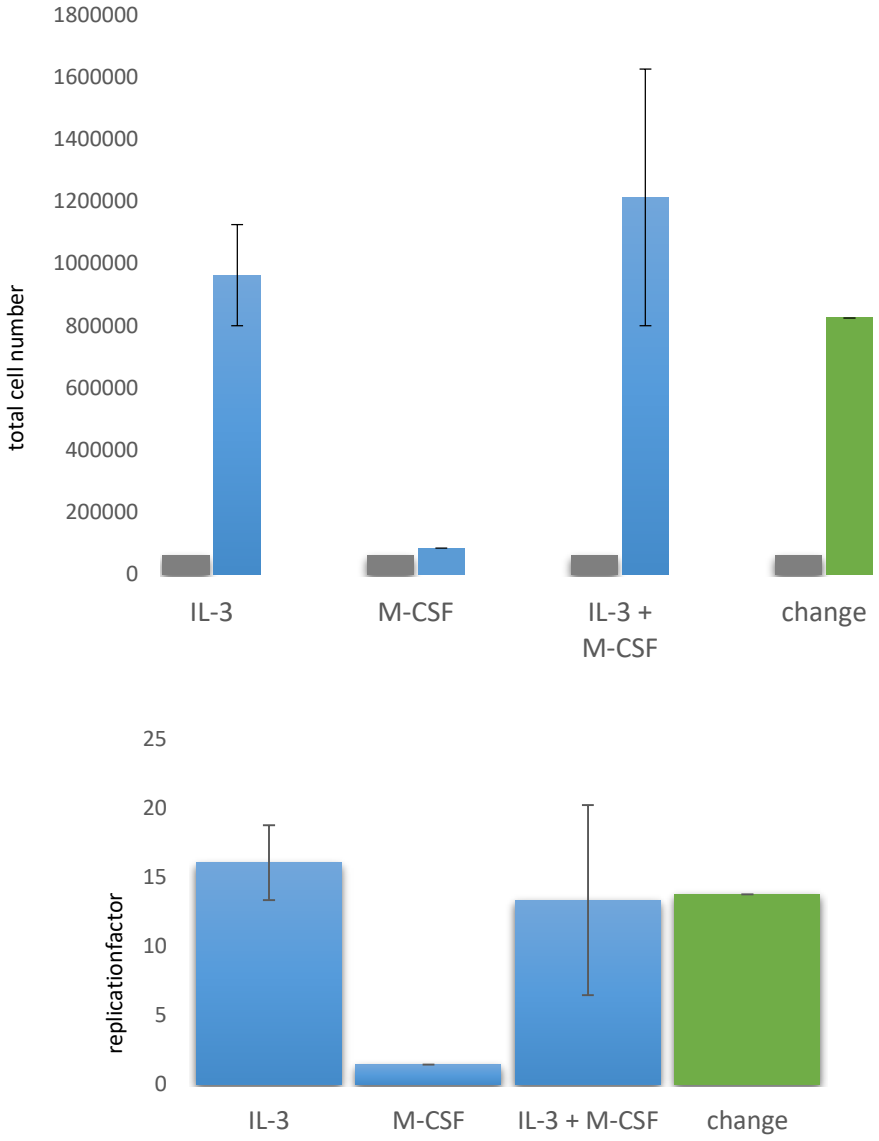

Figure 12: Schematic view on monocyte differentiation and flow cytometry analysis of monocyte / macrophage differentiation setup in combination with statistical graphs of several independent experiments. Two time-points were chosen to harvest the cells and stain for macrophage / monocyte CD33+/CD14+ markers. (A) In panel 1 the IL-3 condition at the first harvesting time-point is shown as an example. Dead cells were excluded with DAPI staining. Living cells were divided into CD33+/CD14- and CD33+/CD14+. These subsets were further analyzed for CCR5 and CD4 expression. (B) Monitoring of monocyte differentiation: monoblasts (CD45+), pre-Monocytes (CD45+/CD33+) and monocytes (CD45+/CD33+/CD14+). (C) Up to three different experiments were compared and plotted in order to choose the most efficient medium. The bars show the different distribution of subsets at either the first or the second time-point in each medium condition. (D) Cell size for each medium condition was monitored via flow cytometry at the first as well as at the second harvesting time-point using the forward scatter. The size is shown in two histograms, one for each time-point, displayed over each other. (E) All four different media were evaluated in terms of proliferation potential at the first harvesting. Shown are the total cell number at the first harvesting and the replication-factor which indicates how often the cells replicated. The grey bars in Panel 1 represent the starting material of proliferation with a number of 60,000 cells. In Panel 2 the replication factor is calculated: the total cell number at the time-point of harvesting is divided by the initial cell number at seeding.

4.5 CCR5 EXPRESSION DURING MONOCYTES/ MACROPHAGES DIFFERENTIATION

Similar to the T cell differentiation analysis, the manifestation of CCR5 on the earliest differentiation stage of monocytes/macrophages was monitored.

In all four media conditions a very similar result was displayed: CCR5 is highly expressed on CD33/CD14 double positive cells but hardly on CD33 single positive cells (see Figure 13). The plot shows the percentage of CCR5 in either CD33 or CD33/CD14 positive cells. A maximum of 72% of the CD33/CD14 double positive cells expressed CCR5 on their surface in the "change" condition. On the opposite, only 15.7% CCR5, which was also the maximum detected for single positive cells overall, could be found on single positive cells in "change" condition. A difference of 56.3% between the two subsets strongly indicates that CCR5 is barely expressed on single positive cells, but well on double positive ones.

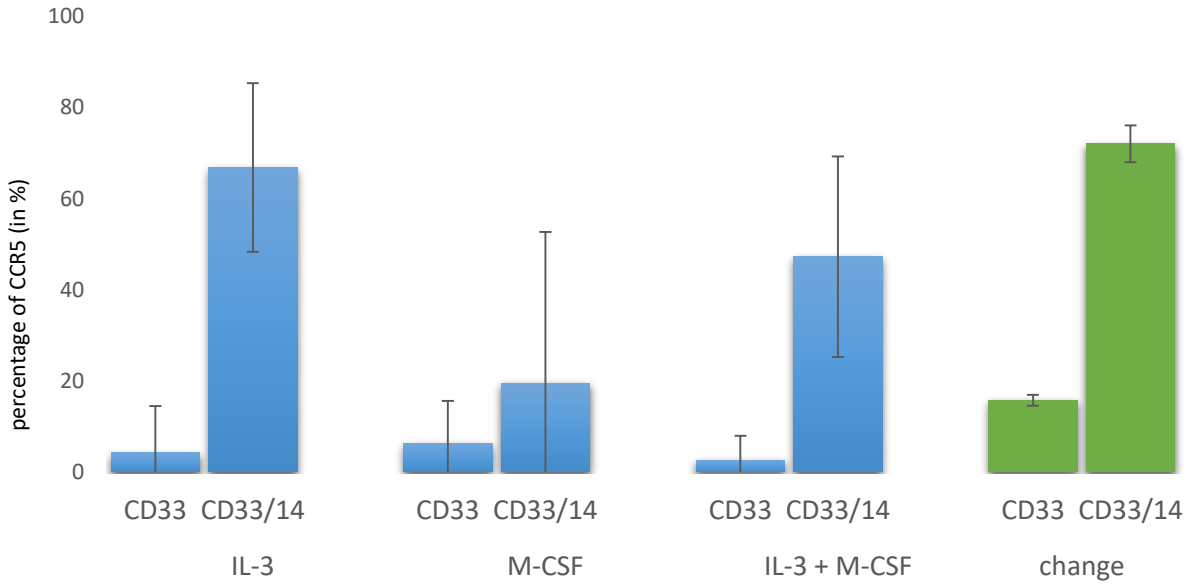

Figure 13: Statistical analysis of CCR5 expression in monocyte/ macrophage progenitors measured by flow cytometry of three independent experiments for IL-3 and IL-3 M-CSF, two independent experiments for M-CSF and one single experiment for change. The bars show the median CCR5 in either in CD33 single positive or CD33/CD14 double positive cells on both harvesting time-points.

4.6 NUCLEOFECTION-EFFICIENCY

In order to evaluate the nucleofection and simultaneously the efficiency of mRNA delivery and expression, cells were nucleofected with GFP mRNA.

One day after nucleofection GFP treated cells were harvested and stained with DAPI. Figure 14 (A) is representing flow cytometry data, three panels which depict the nucleofection-efficiency are shown. In the first panel the vital population of $CD34^+$ cells based on forward and side scatter was selected. The gate of the second panel excludes all cell fragments and dead cells. Finally, in the third panel the GFP positive cells were gated. The mean percentage of living cells over three experiments was 84% (B). On the vast majority of the cells (98.8%, see Figure 14 (B)) a green fluorescence signal could be detected.

The numbers above show that nucleofection was not only very efficient but also very well tolerated by the cells.

A

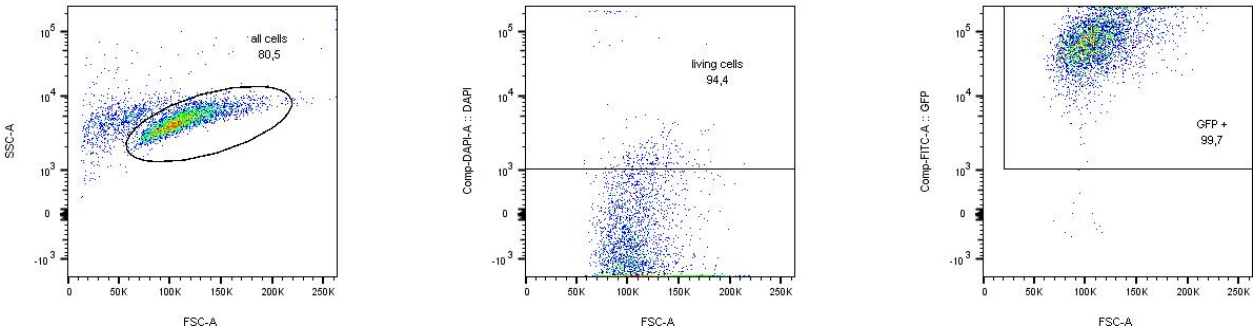

B

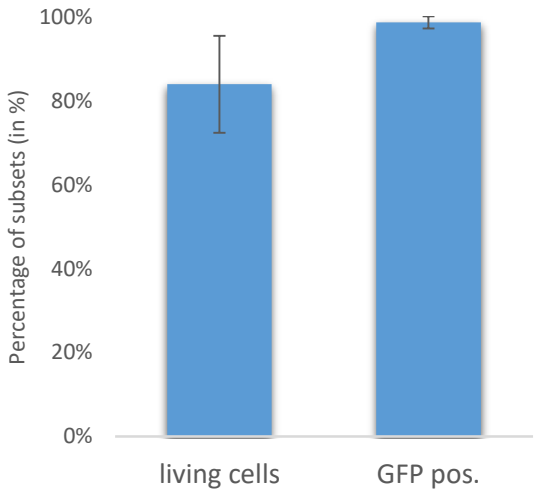

Figure 14: Flow cytometry Analysis of CD34$^+$ cells one day after nucleofection. (A) The first gate was set on the FSC and SSC, the second gate excludes dead cells and debris. In the third panel all cells captured by the gate are GFP positive. (B) The average over three experiments of all living cells as well as the GFP$^+$ cells is shown.

4.7 T CELL DIFFERENTIATION OF MODIFIED STEM CELLS

In 4.2 the results of the differentiation of untreated $CD34^+$ stem cells derived from cord-blood was presented. In Figure 15 the comparison of untreated and TALEN treated cells is shown.

$CD34^+$ stem cells from cord blood were genetically modified before starting the process of differentiation. RNA of a right and a left TALEN were delivered to the cells by nucleofection. Analog to the TALEN treated cells, untreated cells from the same donor were differentiated following the same protocol.

All four subsets identified above in 4.2 could be detected again in the graph of the edited cells (see Figure 15). Each corner of the square represents one particular subset. The percentage interval starts with 0% at the centre of the graph and ends with 80% at the outer square. Each week is represented by a different colour and a dot is drawn in each corner according to the percentage of the subsets. All dots are connected and a unique pattern is created. Every week is represented by one of these patterns. The graph reflects two independent experiments of two different donors.

The characteristic cells for week 1 are the ETP. The percentage of this subsets is in the setup of untreated cells 12% and in the sample of treated cells 16%. Pre-Ts, are compared to later weeks, barely present in week 1 (untreated: 14%; treated: 13%). The Pro-T cell subset is higher in the untreated (41%) than in the treated setup (27%). ISP-DP are either 31% in the untreated or 42% in the treated samples.

Week 2 shows generally less ETP (untreated: 4%; treated: 7%) than week 1. Also the subset of Pro-T cells decreased. This subset is represented by 28% in untreated cells and 18% in treated cells. The subset distribution shifted and the greatest percentage of cells can be found in the Pre-T subset. In the untreated setup 55% of Pre-T cells and in the treated 54% were observed. ISP-DP decreased to 10% (untreated) and 18% (treated).

The trend of an increasing number of Pre-Ts starting at week 2 continued in week 3. 67% of untreated cells and 60% of treated cells appeared to be Pre-T cells. From the third week on, ETP are hardly found anymore (untreated: 2%; treated: 2%). A decrease in percentage is observed in the subset of Pro-T cells. In the untreated setup this subset has 12% and in the treated setup 17%. Finally ISP-DP start increasing from this week on (untreated: 16%; treated: 17%).

In the last week (week4), there is almost a 50:50 distribution of Pre-T cells and ISP-DP. While the untreated setup shows 55% of Pre-T cells and 42% of ISP-DP, the treated setup shows 42% (Pre-T) and 47% (ISP-DP). Both the subsets of ETP (untreated: 2%; treated: 3%) and Pro-T (untreated: 2%; treated: 3%).

This clearly demonstrate the shift of the subsets during differentiation, and that edited cells could be differentiated similarly to the untreated cells.

A

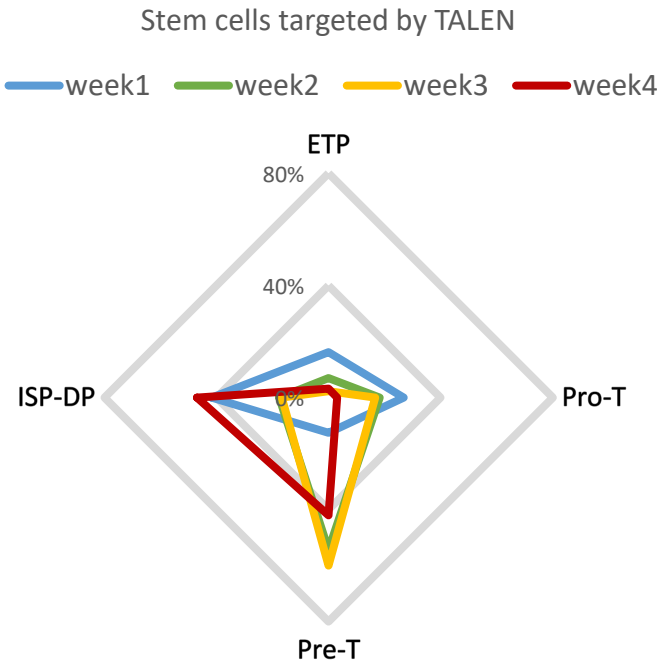

B

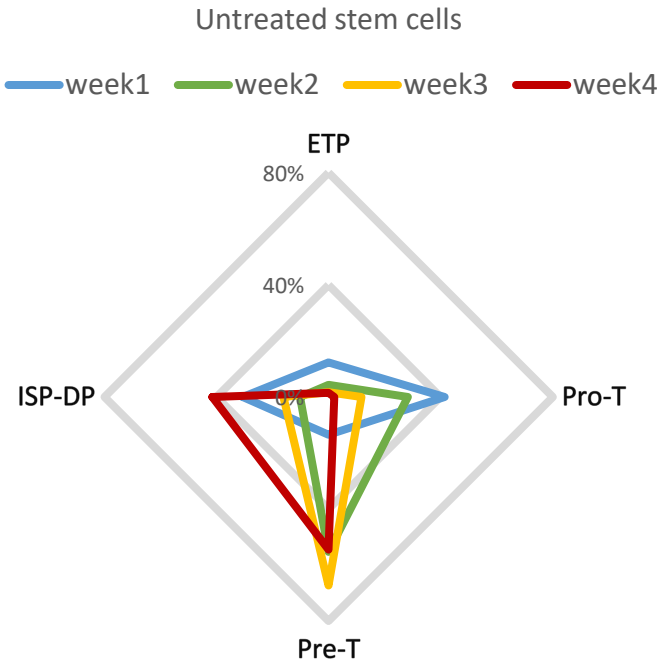

Figure 15: Differentiation subsets of untreated and genetically modified cells. The four corners represent the four subsets in the course of differentiation. For each week a dot representing the percentage of cells in this certain subsets is displayed. All dots are connected and a unique pattern is created which can be easily compared to another. (A) Differentiation subsets of TALEN treated stem cells. (B) Differentiation subsets of untreated stem cells.

4.8 MONOCYTE/MACROPHAGE DIFFERENTIATION OF MODIFIED STEM CELLS

As done with the T-cell differentiation experiment, proof for a normally differentiation process of TALEN treated cells had to be performed as well.

According to the results of the established differentiation protocol (see 4.4), the two conditions in which satisfying cell numbers could be assessed were chosen: IL-3 and IL-3 + M-CSF were used to check for the differentiation potential of CCR5 edited cells. In contrast to the established protocol in the direct comparison of untreated and treated cells, CD4 was also stained. As CD4 is highly necessary for HIV entry (see 1.2) the detection of $CD33^+/CD14^+/CD4^+$ cells will be very informative. These cells represent the actual target cells of HIV. An untreated as well as a treated sample were kept at each condition in culture for 10 days.

In the medium supplemented with IL-3 only, in both untreated and treated cells almost the same percentage of $CD33^+$ cells was observed (untreated: 86%; treated: 90%). Less cells were $CD33^+$ and $CD14^+$ (untreated: 13%; treated: 9%). From these double positive cells in the untreated setup, 70% were additionally $CD4^+$ and 90% were $CD4^+$ in the treated samples (see Figure 16).

When IL-3+M-CSF were supplemented, 72% of the untreated and 94% of the treated cells were $CD33^+$. 27% (untreated) and 6% (treated) could be found in the $CD33^+/CD14^+$ subset. Based on this subset in the untreated setup 58% and in the treated 61% were also $CD4^+$.

In the end both untreated as well as TALEN treated cells were able to differentiate into more mature cells. Treated cells showed not only the general ability of differentiation, they also showed a very similar distribution of cell subsets during the process.

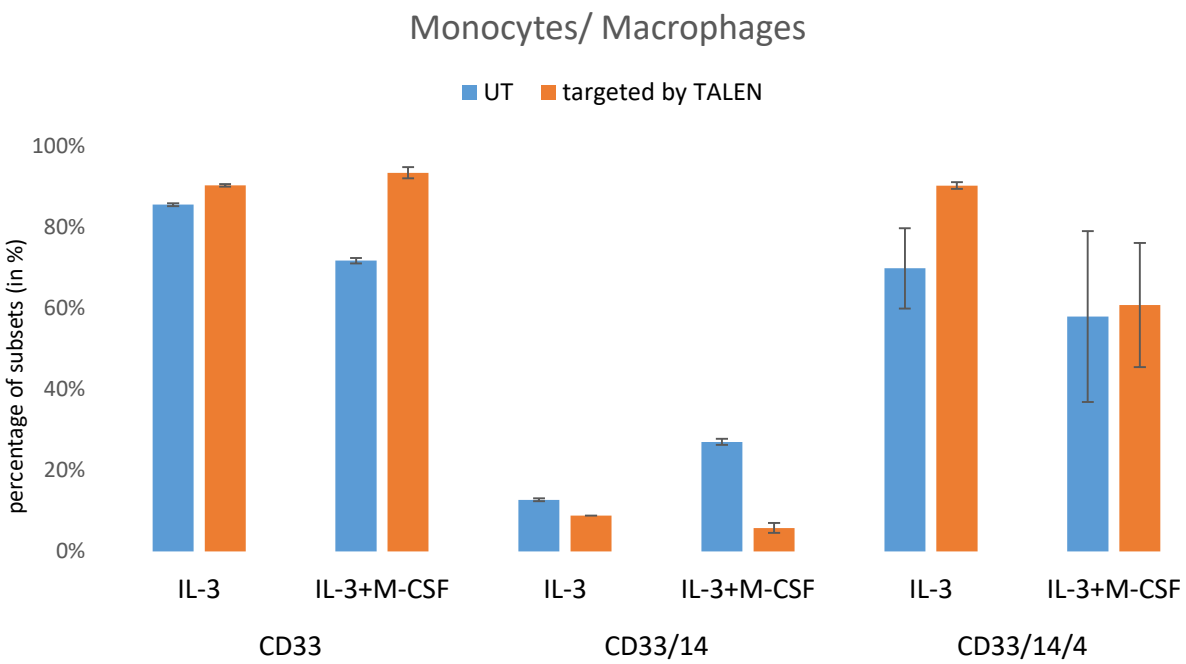

Figure 16: Analysis of monocyte/ macrophage development from flow cytometry data collected in two independent experiments. Each condition (IL-3 and IL-3 + M-CSF) is divided in an untreated and a treated setup. 3 populations are shown: CD33+, CD33+/CD14+ and based on the double positive subset CD33+/CD14+/CD4+.

4.9 CCR5 EXPRESSION IN MODIFIED AND UNTREATED T CELLS

During the course of differentiation the CCR5 status was monitored at each measurement time-point by flow cytometry analysis. Additionally to the staining which detects CCR5 on the cell surface and therefore reflects the phenotype, a test on the genomic level was performed. Some of the cells were harvested, the DNA was extracted, CCR5 locus was amplified and a T7E1-Assay (see 3.10, Figure 8) was carried out.

In contrast to the differentiation staining, CCR5 staining seemed to be very donor dependent. The level of CCR5 varied so strongly that it has not been possible to summarize the data in a statistical analysis.

For both untreated and treated samples, the analysis on the surface expression of CCR5 was performed in the subset of all living cells. The flow cytometry data (Figure 17 (A)) showed that especially beyond week1, a higher number of CCR5 positive cells in the treated samples than in the untreated were present. At the beginning in week 1 the untreated setup showed 30% and the treated setup 32% of CCR5 positive cells. In week 2 the percentage of cells expressing CCR5 on their surface reached 12% in treated and 23% in untreated cells. Week 3 showed 7% of CCR5 positive cells in the treated setup and 16% in the untreated one. Finally at the last measuring-point only 2% in the untreated and 4% in the treated setup could be detected to be CCR5 positive.

The trend visible during the differentiation is a decrease of CCR5 positive cells as well in treated as in untreated cells. Generally a higher amount of CCR5 positive cells could be detected in the treated setup, which was not expected.

Panel B of Figure 17 shows the genomic analysis of the CCR5 locus. Each week a treated sample was analysed along with a control of untreated cells which had not been nucleofected with TALEN mRNA. From week 1 to week 4 the untreated samples showed as expected only this one band. In samples modified by TALEN two fragments appeared on the gel. The intensity of this two bands in relation to the uncleaved top band indicated the percentage of cleavage. During the whole process of differentiation the cleavage efficiency remained constant between 72% and 80%.

A

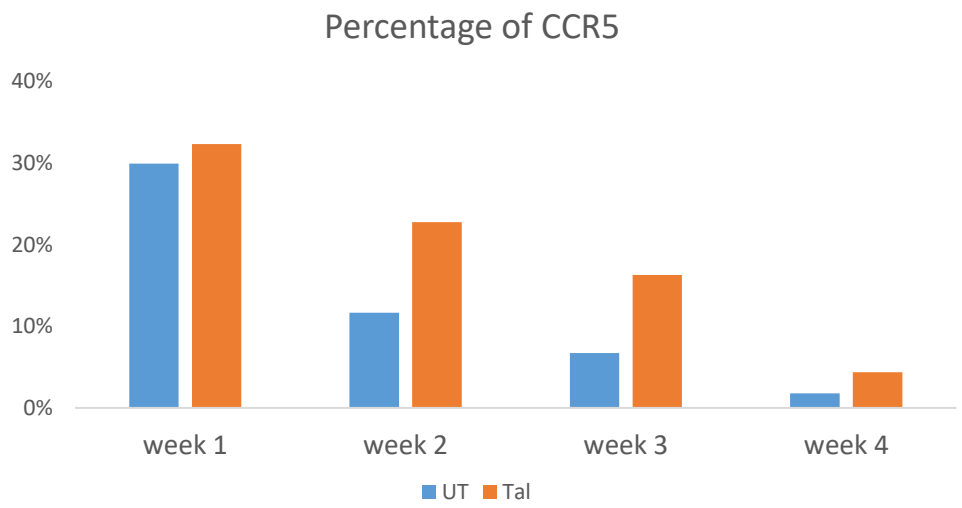

B

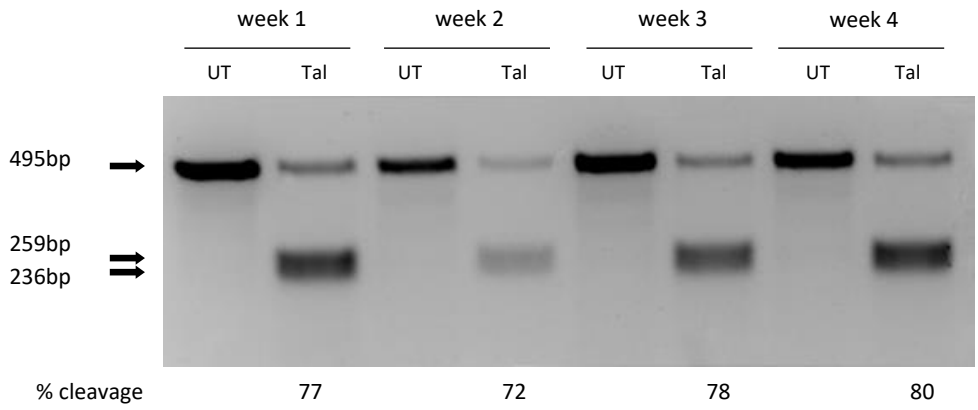

Figure 17: Statistical analysis of CCR5 collected by flow cytometry and T7-Assay data. (A) Expression in untreated and TALEN targeted T cell progenitors measured by flow cytometry. The bars show the percentage of CCR5 in all living cells over the whole period of differentiation (4 weeks). (B) Gel of T-7 Assay performed on cells at each time-point for measurement. In each week a sample of untreated (UT) and TALEN treated cells (Tal) were analyzed via T7-Assay.

4.10 CCR5 EXPRESSION IN MODIFIED AND UNTREATED MONOCYTES/ MACROPHAGES

In parallel to the T cell differentiation, the CCR5 co-receptor was tracked in the monocyte/ macrophage experiment. In contrast to the T cells, only one measuring point was chosen (see 4.4) and two different conditions in the differentiation protocol were used.

In the first panel of Figure 18 (A) the percentage of CCR5 in three different subsets is plotted. This first subset consists of all living cells (dead cells and debris were excluded). From all living cells either all CD33 single positive or all CD33/14 double positive cells were analyzed.

In the samples with IL-3 only 4% (untreated) and 2% (treated) of CCR5 positive cells were found. $CD33^+$ cells showed a low CCR5 in both untreated (2%) and treated (1%) samples. The highest percentage of CCR5 could be found in the $CD33^+/CD14^+$ cells. 25% of these double positive but untreated cells expressed CCR5 on their surface. In the setup of genetically modified cells, 11% of CCR5 positive cells were observed.

When IL-3+M-CSF was supplemented to the medium, 11% of the untreated cells and 2% of the treated cells showed a CCR5 surface expression. In the CD33 subset the CCR5 was detected on 2.3% of the untreated and on 1.6% of the treated cells. Again the highest number of CCR5 positive cells was found in the $CD33^+/CD14^+$ subset. 39% of all untreated double positive cells and 17% of all treated double positive cells were found to be CCR5 positive.

DNA of cells grown in each condition (IL-3 only and IL-3+M-CSF) was harvested and analysed. In both samples the TALEN mRNA treated cells showed a significant cleavage of more than 80% while the untreated controls did not show any cleavage at all (see Figure 18 (B)).

Contrary to the T cell experiment for the monocyte/macrophage differentiation the flow cytometry data harmonized with the T7E1-Assay. Both analysis described a reduction of CCR5 in cells derived from genetically modified $CD34^+$ stem cells.

A

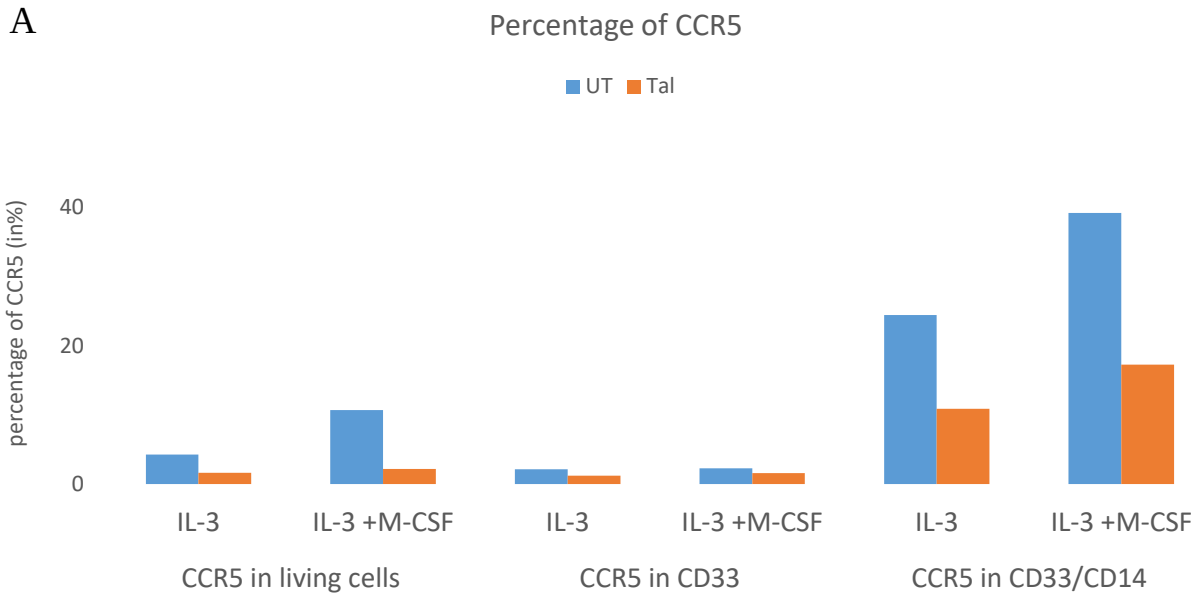

B

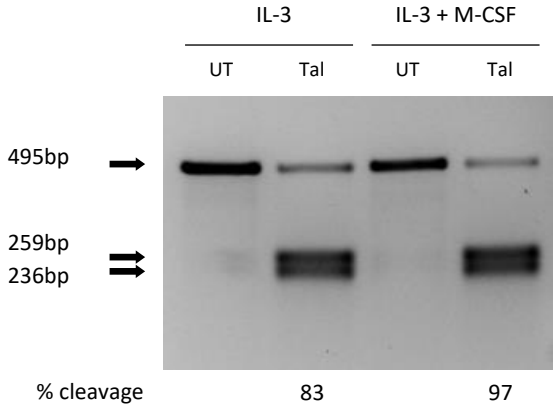

Figure 18: Analysis of CCR5 collected by flow cytometry and T7-Assay data. (A) CCR5 expression in untreated and TALEN targeted monocyte/ macrophage progenitors measured by flow cytometry. The bars show the percentage of CCR5 in all living cells over the whole period of differentiation (4 weeks). (B) Gel of T-7 Assay performed on cells of each condition

DISCUSSION

As mentioned in project goals (2), after the first step of establishing a differentiation protocol the second step was to address the question whether genetically modified stem cells retain their physiological differentiation potential and can differentiate to target cells.

5.1 CORD BLOOD EVALUATION

The amount of nearly 80% CD34 and CD38 double positive cells in a population of stem cells isolated from umbilical cord blood has been observed before. Almost the same distribution of CD markers as shown in chapter 4 was found by L.Chan et. al. - although they extracted these cells for other purposes (55). The high expression of CD38 together with CD34 is characteristic for healthy haematopoietic stem cells and indicates the potential of these cells to differentiate in either myeloid or lymphoid lineage (56), whereas the smaller proportion of CD34+ CD38- cells represent a more primitive stem cells subpopulation. Figure 9 shows that CCR5 is not expressed on cord blood derived stem cells. The percentage of 1.76% CCR5 positive cells is negligible and could possibly be background from an unspecific staining reaction.

5.2 T CELL DIFFERENTIATION

The gating strategy shown in Figure 10 initially excluded all CD4/CD8 double positive cells because T cell progenitors are known to neither express CD4 nor CD8. Cells cannot be differentiated into CD4 or CD8 positive cells within a period of one or two weeks.

The general ability to differentiate CD34+ stem cells into precursors of T cells is shown in Figure 10. The cells performed a cycling from CD34+/CD7- to CD34+/CD7+ to CD34-/CD7+ and finally to CD34-/CD7-, corresponding to the transition from ETP to ISP-DP cells. Most of the cells in one subset underwent this cycling synchronically, that is why the subset of Pro-Ts shows high numbers in week 2: Pro-Ts from week 1 moved on in the process of differentiation and could therefore be found in the subset of Pre-Ts at week 2. Nearly all Pro-Ts had become Pre-Ts and the subset of Pro-Ts decreased in week 2.

Additionally to the tracked CD markers, the average cell size within the lymphocyte population (Figure 10 (D)) gives a hint for the differentiation stage. The antibody stainings strongly suggest a greater number of differentiated cells in week 3 and 4. This finding is supported by the greater cell size observed in week 4 contrary to week 1. Early blood cells appear larger due to high transcription and translation activities whereas more mature cells and direct T-cell precursors are known to be small cells.

Contrary to the expectation of gaining ISP-DPs earliest at late time-points of in-vitro differentiation, some of these cells were already present in week 1. As some of these ISP-DPs were negative for all other stained markers the explanation for this observation is that certain cells are blocked in early stages of differentiation. These cells do not express any of the monitored CD markers on their surfaces. In week 2 the blocked cells disappear which causes the decline of ISP-DPs at this time-point (Figure 10 (C)). The cells detected in the ISP-DSP subset in week 1 are not truly ISP-DPs cells. On the contrary, chances are high that the detected cells in the ISP-DP subset in week 3 and 4 were what they had been expected to be: cells in a differentiation stage close to single positive T cells.

Another explanation for high numbers of ISP-DPs in week 1 is that within an inhomogeneous sample of CD34+ stem cells some T cell precursors of high differential stages were already present. These cells were ISP-DPs at week 1 but then died at week 2 due to the lack of sufficient ligands for mature T cells.

In fact, single positive T cells (CD4 or CD8) could never be detected. Starting at week 4 the cell number began to decrease. At harvesting point week 5 (not shown in the figure) almost no T cells could be found anymore. The speculation is that some specific factors might be missing at this time-point in order to generate mature T cells. Another possible explanation is that the premature cells are somehow blocked in their stages. In a T cell differentiation *in-vitro* study S. Hoseini et. al (43) showed a similar finding: immature T cells were blocked in vitro at the Pre-T cell stage.

The speed of the differentiation process varied between the donors. This indicates that there are inter-individual differences in the differentiation potential of stem cells. One donor’s population showed Pre-Ts already in week 2 (Figure 10), another donor’s cells could reach this stage not before week 3 (data not shown).

CCR5 is detectable on the cells' surface for the first time between the Pro-T and Pre-T stage. The percentage of CCR5 on ETPs is comparable to the starting material of $CD34^+$ stem cells which show no expression of CCR5 on their surface at all. Donor specific variations could be found: in one experiment, the Pro-T cells already highly expressed CCR5 and in another experiment CCR5 was found earlier in Pre-T cell. These inter-individual differences cause the high standard deviation shown in Figure 10 (A). In conclusion, all stages before the Pro-T stage are not targetable for HIV in terms of CCR5. Apart from CCR5, the CD4 receptor is mandatory for HIV to enter cells, too. Although CCR5 can be monitored in the generated T cell precursor, these cells are, due to the lack of CD4, no target cells for HIV. Only T cells expressing both CCR5 and CD4 can actually be infected by the virus: mature T cells. Nevertheless, the data shows that CCR5 is present already at early time-points during the differentiation of T cells.

In chapter 5.5 below, the differentiation potential of genetically modified stem cells is evaluated in detail. The experiments demonstrated that CCR5 edited $CD34^+$ cells can undergo the same maturation process as untreated cells. This ability of a sufficient and natural differentiation constitutes the basis of a functional therapy with *ex-vivo* treated stem cells.

5.3 MONOCYTE/ MACROPHAGE DIFFERENTIATION

All of the four tested media conditions described in 4.4 had the potential to generate CD33/CD14 double positive cells (Figure 12). Although the ratio of single positive to double positive cells strongly varied among donors.

M-CSF alone showed the best yield of double positive cells but the differentiated cells hardly proliferated. The low cell number caused the high standard deviation in Figure 12 and Figure 13. Therefore the media condition containing M-CSF only was not very useful to generate many monocyte/ macrophage precursors. By introducing condition "change" the importance of IL-3 for proliferation was clearly visible. In order to show the differentiation of modified $CD34^+$ cells into macrophages/monocytes via flow cytometry and molecular biologic methods, a sufficient number of cells was needed. Therefore only the media conditions IL-3 + M-CSF and IL-3 could be used as culturing conditions for this purpose.

CCR5 was already detected at the first harvesting time-point. Figure 13 (A) shows that the earliest time point for CCR5 to be expressed is in CD33/CD14 double positive cells. About 50% (Figure 12 (B)) of these double positive cells were theoretically targets for HIV: these cells were both CD4 and CCR5 positive. In contrast to the T cell protocol (in which CCR5/CD4 positive cells could not be detected) the monocyte differentiation protocol showed the potential to produce HIV targets. These target cells could be used in the future for functional assays such as for example viral challenges.

Contrary to the size distribution observed during T cell differentiation, more differentiated monocytes/macrophages showed a greater size than in earlier differentiation stages. Unlike T cells, monocytes and especially macrophages are known to be large cells. Although haematopoietic precursor cells are highly active in transcription, translation and protein synthesis, mature monocytes/macrophages show a larger cell diameter. HSCs have a diameter of 12µm, the size of monocytes and macrophages is 15-20µm (36). Additionally to the size analysis, a microscopic evaluation of the nucleus could have been performed. Cells with a strong protein synthesis have a big nucleus (36). More differentiated cells are less active in protein translation and the nucleus is expected to be smaller.

5.4 NUCLEOFECTION

Though the concept of nucleofection invented by Amaxa (distributed by Lonza) claims to be more efficient and less toxic to the cells than other electroporation methods, some toxic effects, especially slower cell growth, can still be observed (57). Dr. Giandomenico Turchiano from AG Cathomen has performed several experiments to optimize nucleofection-program for $CD34^+$ primary cells. Each of these programs differ in the applied electric pulses. In many cases the high transfection efficiency of a program was linked to a great loss of viability. As mentioned in "material and methods" I decided to use the program DZ-100. According to Dr. Turchianos results this program was able to combine a good efficiency and high viability. Nevertheless, as presented in Figure 14 one day after nucleofection some toxic effects could be observed. At 24h post nucleofection, the viability staining performed via flow cytometry analysis showed toxicity, as well as directly looking at the cells through a light microscope confirmed that the cells underwent great stress. Instead of round and chubby, the cells had irregular-shaped membranes and appeared

ragged. Nevertheless the efficiency of mRNA delivery was highly satisfying and the viabilities improved over time, as the cells recovered. The control cells (see Figure 14) nucleofected with GFP mRNA internalized the mRNA and started producing GFP with efficiencies close to 100%. As a clear population with a strong green signal could be detected one can assume that also the TALEN RNA was delivered with similar efficiency to the target cells.

5.5 T CELL DIFFERENTIATION OF MODIFIED STEM CELLS

During differentiation both setups (untreated vs. TALEN treated) underwent the same cyclic expansion and decreasing of subsets. The untreated as well as the TALEN treated cells showed ETP only in week 1, a high number of Pro-T cells in week 1 and week 2 and an increase of Pre-T cells from week 2 to week 3 which then dropped in week 4 in favor of ISP-DP.

The percentage of each untreated and treated subsets especially differed mainly in the first and already less in the second week. From the third week on, the development and the percentage of subsets was more or less identical. This trend can be summarized as following: the later the week the more similar the treated sample became to the untreated. The explanation for this trend is that the nucleofection triggered great stress to the stem cells. Also, the internalization of mRNA might have had a negative influence on the cells: in fact, the control cells nucleofected with GFP mRNA showed some stress as well. Pulsing the cells without mRNA also stresses the cells, albeit to a lesser degree (not shown). So the combination of pulse and mRNA delivery increased toxicities. Nevertheless a certain amount of time was needed for recovery. Already at week 2 the negative effect of the nucleofection seemed to vanish. In week 1 the percentage of ETP was a little bit higher in the treated (16%) than in the untreated (12%) setup. This fact was complemented by the number of Pro Ts. Untreated cells were able to give rise to 41% Pro-T cells already in week 1. The TALEN mRNA nucleofected cells instead showed only 26% Pro-T cells (see Figure 15). As ETP represent the direct progenitors of Pro-T cells this lead to the conclusion that nucleofected cells were just a little bit slower than the untreated controls. As previously mentioned, this reflects a period of recovery where the cells seemed to deal more with cell repair mechanisms than with differentiation.

Another hint as of why the subset-percentages in week 1 and 2 showed a deviation, is the absolute cell number. Although more cells (120,000 vs. 100,000) were used for the nucleofection setup than for the untreated one, after nucleofection the cell number was lower in the treated sample (due to

the nucleofection toxicity). In order to minimize cell manipulation this was not determined by the nucleocounter but by eye via the light microscope. As not only the cytokines in the medium but the cellto cell interactions do play an important role in T-cell differentiation (58), the concentration of cells likely influences the potential of differentiation. As the toxic effect was decreasing over time and also the cell numbers became more equal between untreated and treated till week 4, the percentage of subsets became more similar.

The similar distribution of cells in the different subsets at week 4 indicates that in fact CCR5 knock-out cells are able to differentiate into T cell precursors. It might be necessary to find a less stressful way for mRNA delivery and further improve the pulses in order to enhance the differentiation potential of the stem cells already from the beginning. Further efforts have been put toward these improvements in the lab.

5.6 MONOCYTE/ MACROPHAGE DIFFERENTIATION OF MODIFIED STEM CELLS

When comparing untreated and treated $CD34^+$ stem cells after 10 days in IL-3 more $CD33^+$ cells are found in the treated setup than in the untreated one (see Figure 12). This observation is true for IL-3 as well as for M-CSF. In this condition the difference (=22%) between untreated and treated appeared even more clearly. To understand this, one has to consider the percentage of the $CD33^+/CD14^+$ subset. On the contrary more double positive cells formed here from the untreated stem cells than from the genetically modified ones. Again, especially if both (IL-3 + M-CSF) supplements were used the difference was even more convincing (IL-3: 4%; IL3+M-CSF: 21%).

Condition IL-3 and M-CSF had the potential to produce more $CD33^+/CD14^+$ double positive cells. Similar to the T cell differentiation, nucleofected cells seemed to be a little bit slower in differentiation. The higher percentage of $CD33^+$ single positive in the treated cell setup in combination with a lower percentage of the $CD33^+/CD14^+$ double positive subset reflects this fact. The theory, that a certain recovery time is needed after the nucleofection, is also applicable for the differentiation in monocytes/macrophages.

Interestingly, treated stem cells show a higher percentage of $CD33^+/CD14^+/CD4^+$ cells than untreated. As there were more $CD33^+/CD14^+$ positive cells in the untreated setup there were as well more cells somewhere in between $CD33^+/CD14^+$ and $CD33^+/CD14^+/CD4^+$. This idea is based

on the concept that if one cell once started the differentiation this cell efficiently moves on the triple positive stage. The more cells are performing this development the more cells can be detected somewhere between the stages. These cells might appear still in a lower subset though on the move to a higher one.

Additionally, the absolute cell number may give an explanation as well. The samples derived from TALEN targeted cells had always a lower cell number than the untreated controls. There might be some block by the CD4 cells for other cells to become $CD4^+$, too. Especially in the IL-3 + M-CSF condition where more $CD33^+/CD14^+$ cells were found than with IL-3 only, were less $CD4^+$ cells were detected. As the size and therefor the volume of the wells were kept the same with each sample, a higher absolute number of $CD4^+$ cells (in the TALEN treated sample) would have also raised the concentration of "blocking ligands". This theory of course assumes that the culturing dish reflects a microenvironment which regulated its cell composition independently.

Directly compared, both conditions with IL-3 only and IL-3+M-CSF showed similar results. In terms of the ability to generate triple positive ($CD33^+/CD14^+/CD4^+$) cells treated with IL-3 only seemed to work slightly better in both treated and untreated cells. In the untreated cells the IL-3+ M-CSF condition gave rise to 14% more double positive ($CD33^+/CD14^+$) cells than IL-3 alone. In samples with TALEN targeted cells, a difference between both conditions was hardly to determine (except triple positive cells). If a functional assay is planned and target cells for HIV in are required, because of the better yield of $CD4^+$ cells, Il-3 only condition would probably the condition to be favoured. In order to assess the differentiation potential of stem cells both media conditions are equally efficient.

5.7 CCR5 IN MODIFIED AND UNTREATED T CELLS & MONOCYTS/ MACROPHAGES

Both Figure 17 and Figure 18 show a sufficient modification of the differentiated cells on the genomic level.

In the T cell differentiation experiment the percentage of cleaved CCR5 was in week 1, 3 and 4 higher than 75%. The lower percentage of cleavage in week 2 was probably caused during the evaluation process and not by the genotype of the cells (Figure 17). The most probable explanation is that while loading the gel some DNA was spilled. This theory corresponds to the fact that not

only the two cleaved bands are lower in intensity but also the upper uncleaved band seems to be weaker in comparison to the bands of week 1, 3 or 4.

The T7E1-Assay performed from samples of monocyte/macrophage precursors show an even higher percentage of cleavage in the gel. 83% of cleavage in cells of samples with the supplementation of IL-3 only and even 97% of cleavage in cells grown in a medium with IL-3 and M-CSF was detected.

As mentioned before (see 3.10) the evaluation of the T7E1-Assay gels was performed with a software which analyses the pictures of the gel and calculate the density of the pixels. Although a ratio between uncleaved and cleaved bands is calculated, the saturation of the gel image plays an essential role. As the gels were not exposed for exactly the same time under UV light, slight differences of saturation are likely to be found. Additionally a bias during the analysis of the pictures by using a software may have occurred. The calculations of ImageJ are not fully automated. Although each measurement has been performed three times, each user can chose different parameters and settings in the software. Therefore the concrete number of cleavage-percentage has to be evaluated carefully. Also, resolution of T7E1-Assay lies in the 5% range, therefore variation within this range are expected. Nevertheless the overall trend is clearly visible: $CD34^+$ edited stem cells keep their genotype during the differentiation towards their final cell type. This data strongly suggests that the mature cells will remain stably modified.

Theoretically, if the CCR5 co-receptor gene is knocked out, the surface expression level of CCR5 protein on the targeted cells should be reduced. A hypothetical genomic knockout of 100% would then as well lead to a 100% reduction of surface CCR5, whereas a more realistic 90% KO would give rise, according to a statistical distribution of the alleles, to 81% of biallelic mutations, 18% of monoallelic mutations and a remaining1% of wt cells. The cells carrying the monoallelic mutation will still be able to express CCR5 from the wt allele, albeit to a lesser degree, but still theoretically allowing HIV to enter the cell. Considering the Indels length as random, 1/3 of these events will correspond to an insertion or deletion that will not disrupt the CCR5 reading frame. This was confirmed by deep sequencing data (collected by Markus Hildenbeutel AG Cathomen).These findings mean that the mRNA of the protein is transcribed and if this new mRNA is stable, translation takes place as well. Surely, this modified CCR5 co-receptor is not identical with the wild type but depending on where the mutation occurred it might be still sufficient to reach the

membrane and for an antibody or even HIV to bind. To reduce this chance the coding sequence of the N-terminal region was chosen as TALEN target, thus promoting a truncation of the protein right at the beginning after the first 10 amino acids. The target region codes for several tyrosines and acidic amino acids which are used as binding region by HIV, (34). Also, the antibody chosen for the CCR5 staining was specific for this region.

Although the 3A9 clone which was used as antibody, binds to an epitope identically to the deleted region, C. Königs et. al (59) mentioned that this clone has the potential to slightly bind to other regions as well, such as the extracellular loop 1 and 3 of the CCR5 protein.

The fact that CCR5 expressing cells are still found in both TALEN treated stem cells derived T cells and monocytes/ macrophages, might be based on the factors mentioned above: the CCR5 co-receptor is still expressed as some of the deletions caused by the TALEN are not completely abrogating protein expression. The protein fragment on the surface exhibits structures to which the antibody binds and a signal is detected in the flow cytometry analysis. This does not necessarily mean that the mutated CCR5-coreceptor can be used for HIV entry efficiently, but it does also not proof the opposite.

The explanation for a high number of CCR5 positive cells in the T cell precursor setup, especially in the treated compared to the untreated cells, might be caused by a weak point of the 3A9 clone. A cross reactivity of this clone between CCR5 and CCR8 is described (60). As CCR8 is reported to be involved in inflammatory events (61), this receptor could be potentially upregulated in T cell precursors due to the stress caused by the nucleofection and the mRNA. As monocytes/macrophages are part of a completely different cell lineage (lymphoid vs. myeloid) CCR8 might not be expressed in these cells to the same extend. CCR8 was found on a special T cell subset of $CD4^+$ and $CD8^+$ T cells as well as on monocytes and especially on dendritic cells. On the surface of $CD8^+$ T cells CCR8 is strongly upregulated after T cell activation (62). Although no $CD8^+$ cells could be detected in my differentiation experiment (data not shown) it is not impossible that already precursor T cells have the potential to upregulate CCR8.

Ideally the staining for CCR5 should be linked with the simultaneous detection of CCR8. In this way the signal could be clearly assigned. Because of the lack of time I was not able to set up an experiment to address this question. As my goal was to show the differentiation potential of TALEN treated stem cells this matter was of second priority.

5.8 FURTHER EXPERIMENTS

The experiments which I have reported showed that $CD34^+$ stem cells derived from cord blood are indeed able to differentiate in vitro. Progenitors of the final cell type keep their genomic status: the cleavage observed in the stem cells persisted until the final stages which were observed in this artificial differentiation. This fact indicates that also the patient who is treated with CCR5 knock-out stem cells, will potentially be able to obtain mature cells from these transplanted stem cells. In the patient organism, the fully differentiated cells will ideally still carry the mutation in the CCR5 gene.

Apart from the genomic characteristics also the phenotype of the T cell and monocyte/ macrophage precursors was analysed. In the monocyte/macrophage experiment a reduced CCR5 expression compared to the control was not only deducted from the T7E1-Assay but also via flow cytometry. Although reduced, some CCR5 signal could still be detected on the cell surface. As discussed in 5.7 this might not truly be a signal of CCR5 but could also represent CCR8. In order to sort out this observation as well as the contradictory results of the CCR5 staining on T cell progenitors a new round of differentiation should be started in which CCR5 and CCR8 are simultaneously tracked. In this way more definitive information about the phenotypic receptor status can be acquired.

The next step after *in-vitro* differentiation is a verification in mice. Are the transplanted cells able to engraft? Will the host immune system accept these new cells? Are CCR5 knock-out cells able to persist constantly in a foreign organism? Some hints to answer this questions were already given by Li et al. in 2013. In NOD.Cg-Prkdc^{scid}IL2rgt^{m1WJI}/SZJ (NSG) mice ZFN-treated haematopoietic stem cells were transplanted and an engraftment of the $CD34^+$ could be observed. Also, descendants of the transplanted stem cells like $CD4^+$ and $CD8^+$ T cells, B cells and monocytes could be found in these mice (63). This data proves that the concept of modified stem cells engrafted in foreign hosts is valid. Not only stem cells treated with ZFN, but also cells treated with TALEN should be able to show engraftment. Indeed, mice experiments performed in our lab indicate that engraftment and differentiation are possible, as well as stable genomic disruption.

Before moving forward to a clinical application, functionality assays have to be performed. The knowledge that genomic engineered and transplanted stem cells can differentiate physiologically is of course only useful if the modification has been successful. At the moment in the Cornu lab

functional assays with pseudotyped lentiviral vectors and wt HIV have been performed on terminally differentiated edited CD4+ cells, derived from peripheral blood. Functional assays for edited stem cells are still missing: a challenge with HIV to address the question whether the CCR5 knockout is sufficient to trigger entry inhibition of the virus. Ideally $CD33^+/CD14^+/CD4^+$ monocyte/macrophage precursors are sorted by flow cytometry and isolated. These cells closely represent actual HIV target cells. After isolation, the target cells will be challenged with either a lentiviral vector which acts as surrogates for HIV-1 and is pseudotyped with the R5 tropic HIV glycoprotein and expresses the marker protein GFP, or directly challenge the cells with the actual wt HIV virus.

Additionally, instead of *in-vitro* differentiation approach, the mouse model needs to be evaluated. Mice with engrafted $CD34^+$ stem cells carrying high knockout-rates in the CCR5 gene will be challenged with the virus itself. Facilities that perform this kind of experiment are not available in Germany. Both challenges will prove if the reduction of CCR5 is high enough to establish a sufficient immunity against HIV.

Every drug has its specific side effects. In the case of designer nucleases off-target events are considered as side effects. Sequences similar to the actual target might be cleaved by the used TALEN as well. As long as these off-targets appear in unimportant parts of the genome no negative effects will be observed. If however tumor suppressor genes are harmed, severe consequences can be caused to the patient. For the pair of TALEN I have used, one off-target was found in an intron. After verifying this off-targets by deep sequencing again in the cells from the mouse model it will be verified if clonal expansion has taken place, although this is a process that might require years, therefore might not be detectable in the mouse setting.

SUMMARY

Today's therapy of HIV offers patients the opportunity to live almost normally. The life expectancy of HIV patients increased dramatically over the last decades. Nowadays patients are hardly restricted in their way of life. Although side effects under ART are still present, a new therapy in order to be revolutionary needs to finally cure HIV. This remaining task is targeted by many new therapy concepts including genome engineering. A broader distribution of drugs as well as a better education on HIV and safe sex are both able to decrease HIV incidence and mortality worldwide, but after all the curative therapy will remain the last resort.

Designer nucleases such as TALEN and CRISPR/Cas9 are highly promising tools to solve the riddle of curing HIV. The efficiency of CCR5 knock-out introduced by TALEN, is already very high. The off-target activity is rather low and the risk of severe or even lethal side effects seem to be minimal. In my studies I set up protocols for the *in-vitro* differentiation for both T cells and monocytes/makrophages. Additionally I produced and then delivered TALEN mRNA to $CD34^+$ stem cells derived from cord blood and proved that if designer nucleases are applied to these stem cells, they are able to differentiate physiologically. I obtained $CD33^+/CD14^+/CD4^+$ monocyte/ macrophage precursors as well as direct T cell progenitors. Especially the monocyte/ makrophage precursors represent actual target cells for HIV and can be used for further functional analysis. Moreover, I have been able to demonstrate that once established in stem cells, the knock-out remains throughout the whole process of differentiation and persists very likely in the finally differentiated mature cells, too. The cleavage efficiencies I observed in the CCR5 locus, ranged between 70% and 97%. This indicates that almost all cells were efficiently genetically modified.

After the protocol for a TALEN based genomic treatment of $CD34^+$ stem cells was introduced and optimized by Emily Meyer in the Cornu lab, I further proved in my studies that the concept of genome engineering HIV target cells by editing their stem cells is at least functional *in-vitro.* This data strongly suggests that the transplanted cells in human are able to support the patient's organism in develooping immune cells. The next experiments will have to deal with the issue of *in vivo* cell differentiation. Furthermore functionality assays have to be performed which show that the concept of CCR5 knock-out cells is valid and really sufficient in inhibiting HIV to infiltrate the organism. Based on these results the new treatment of HIV will be established.

ZUSAMMENFASSUNG

Seit den Anfängen der HIV Therapie hat sich die Behandlung der Patienten insbesondere in den letzten Jahrzehnten stark weiterentwickelt, HIV positive Patienten haben heutzutage weder in ihrer Lebenserwartung noch ihrer Lebensführung mit drastischen Einschränkungen zu rechnen. Dennoch ist es auch heute noch nicht möglich HIV infizierte Patienten vollends zu heilen. Hier müssen die neuen Therapieoptionen, so auch die Gentherapie, ansetzen. Maßnahmen zur Aufklärung über „safe sex“ und HIV, sowie die verbesserte Verteilung von Medikamenten insbesondere in Drittweltländer sind in der Lage die Inzidenz und Prävalenz der HIV Infektionen weltweit zu beeinflussen. Ultima ratio wird aber auch weiterhin die Heilung der Erkrankung bleiben, die nur mit Hilfe neuer kurativen Verfahren realisiert werden kann.

Designer Nukleasen wie TALEN oder CRISPR/Cas9 stellen vielversprechende Werkzeuge im Kampf gegen HIV dar. Die Eliminierung des CCR5 co-receptors, der eine wesentliche Rolle für die Infizierung der Zelle durch HIV darstellt, auf genomischer Ebene lässt sich mit TALEN effektiv durchführen. Ungewünschte „off-targets“ (akzidentiell modifizierte Regionen die nicht der Zielregion entsprechen) werden selten beobachtet. Auch die Wahrscheinlichkeit für toxische Nebenwirkungen erscheint niedrig. Im Rahmen meiner Dissertation konnte ich Protokolle für die *in vitro* Differenzierung von $CD34^+$ Stammzellen aus Nabelschnurblut in sowohl Monozyten/ Macrophagen als auch T-Zellen etablieren. Des Weiteren ist es mir gelungen TALEN mRNA zu produzieren und diese in die Zellen einzuschleusen, um dann zu zeigen, dass genetisch modifizierte Stammzellen ihr physiologisches Differenzierungspotential während dieses Procedere behalten. Die T-Zell Vorläufer und insbesondere die $CD33^+/CD14^+/CD4^+$ Monozyten/Macrophagen gelten als direkte Zielzellen von HIV im menschlichen Organismus. Ergänzend zur Analyse des Differenzierungspotentials zeigen meine Ergebnisse, dass die Zielzellen ihren, im „Stammzellalter“ veränderten, genetischen Status während der Reifung zur erwachsenen Zelle beibehalten. Die knock-out Effektivität im CCR5 locus lag in meinen Experimenten bei mindestens 70% und maximal 97%, diese Zahlen belegen: so gut wie alle Stammzellen sind erfolgreich genetisch verändert worden.

Basierend auf Emily Meyers Erkenntnissen zum erfolgreichen „genome editing“ mittels TALEN in $CD34^+$ Stammzellen in der AG Cornu (33), habe ich mit meiner Arbeit gezeigt, dass zumindest *in vitro* das Konzept zur genetischen Modifikation von HIV Zielzellen über die Bearbeitung deren

Stammzellen funktional ist. Auf Grund dieser Daten kann vermutet werden, dass auch modifizierte Stammzellen, die in den menschlichen Organismus transplantiert wurden, in der Lage sind, funktionsfähige Blut- und Immunzellen zu produzieren. Zukünftige Experimente werden sich mit dieser *in vivo* Differenzierung beschäftigen müssen. Außerdem muss in einem kontrollierten Umfeld überprüft werden, ob die in den Zellen etablierte Modifikation tatsächlich den erhofften Infektionsschutz gegen HIV bietet und damit auch als Grundlage für eine neue Therapie dienen kann.

LIST OF FIGURES/TABLES

REFERENCES

1. Zhu P, Liu J, Bess J, Chertova E, Lifson JD, Grisé H, et al. Distribution and three-dimensional structure of AIDS virus envelope spikes. Nature. 2006;441(7095):847–52.
2. Sharp PM, Hahn BH. Origins of HIV and the AIDS pandemic. Cold Spring Harb Perspect Med. 2011;1(1):1–22.
3. Worobey M, Gemmel M, Teuwen DE, Haselkorn T, Bunce M, Muyembe J, et al. Direct Evidence of Extensive Diversity of HIV-1 in Kinshasa by 1960. 2008;455(7213):661–4.
4. Hemelaar J, Gouws E, Ghys PD, Osmanov S. Global trends in molecular epidemiology of HIV-1 during 2000– 2007. AIDS. 2011;25(5):679–89.
5. UNAIDS. Miles To Go: Closing Gaps Breaking Barriers Righting Injustices. Unaids. 2018
6. Infektionskrankheiten R. Epidemiologisches Bulletin. Epidemiol Bull. 2018;(47):493–510.
7. Quinn TC, Wawer MJ, Sewankambo N, Serwadda D, Li C, Wabwire-Mangen F, et al. Viral Load and Heterosexual Transmission of Human Immunodeficiency Virus Type 1. N Engl J Med. 2000 Mar 30;342(13):921–9.
8. Huang Y, Paxton WA, Wolinsky SM, Neumann AU, Zhang L, He T, et al. The role of a mutant CCR5 allele in HIV-1 transmission and disease progression. Nat Med. 1996 Nov;2(11):1240–3.
9. Klasse PJ. The molecular basis of HIV entry. Cell Microbiol. 2012;14(8):1183–92.
10. Rosen O, Sharon M, Quadt-Akabayov SR, Anglister J. Molecular switch for alternative conformations of the HIV-1 V3 region: implications for phenotype conversion. Proc Natl Acad Sci U S A. 2006;103(38):13950–5.
11. Moore JP, Trkola A, Dragic T. Co-receptors for HIV-1 entry. Vol. 9, Current Opinion in Immunology. 1997. p. 551–62.
12. Kulkarni H, Marconi VC, Agan BK, McArthur C, Crawford G, Clark RA, et al. Role of CCL3L1-CCR5 genotypes in the epidemic spread of HIV-1 and evaluation of vaccine efficacy. PLoS One. 2008;3(11):1–9.

13. Delobel P, Sandres-Sauné K, Cazabat M, Pasquier C, Marchou B, Massip P, et al. R5 to X4 switch of the predominant HIV-1 population in cellular reservoirs during effective highly active antiretroviral therapy. J Acquir Immune Defic Syndr. 2005;38(4):382–92.

14. Balanovsky O, Pocheshkhova E, Pshenichnov A, Solovieva D, Kuznetsova M, Voronko O, et al. Is Spatial Distribution of the HIV-1-resistant CCR5Δ32 Allele Formed by Ecological Factors? J Physiol Anthropol Appl Human Sci. 2005;24(4):375–82.

15. Liu R, Paxton WA, Choe S, Ceradini D, Martin SR, Horuk R, et al. Homozygous defect in HIV-1 coreceptor accounts for resistance of some multiply-exposed individuals to HIV-1 infection. Cell. 1996;86(3):367–77.

16. Quillent C, Oberlin E, Braun J, Rousset D, Gonzalez-Canali G, Métais P, et al. HIV-1-resistance phenotype conferred by combination of two separate inherited mutations of CCR5 gene. Lancet. 1998;351(9095):14–8.

17. Adults H--infected. Guidelines for the Use of Antiretroviral Agents in HIV-1-Infected Adults and Adolescents Developed by the HHS Panel on Antiretroviral Guidelines for. October. 2012;

18. Deutsche AIDS-Gesellschaft (DAIG). Deutsch-Österreichische Leitlinien zur antiretroviralen Therapie der HIV-Infektion Version 7 vom 29.11.2017. 2017;AWMF 055-0:1–43.

19. Hütter G, Ganepola S. Eradication of HIV by Transplantation of CCR5-Deficient Hematopoietic Stem Cells. Opin TheScientificWorldJOURNAL. 2011;11:1068–76.

20. Avettand-Fenoel V, Prazuck T, Hocqueloux L, Melard A, Michau C, Kerdraon R, et al. HIV-DNA in rectal cells is well correlated with HIV-DNA in blood in different groups of patients, including long-term non-progressors. Aids. 2008;22(14):1880–2.

21. Yukl SA, Boritz E, Busch M, Bentsen C, Chun TW, Douek D, et al. Challenges in Detecting HIV Persistence during Potentially Curative Interventions: A Study of the Berlin Patient. PLoS Pathog. 2013;

22. Hütter G, Bodor J, Ledger S, Boyd M, Millington M, Tsie M, et al. CCR5 targeted cell therapy for hiv and prevention of viral escape. Viruses. 2015;

23. Kim J-S. Genome editing comes of age. Nat Protoc. 2016;11(9):1573–8.

24. Rouet P, Smih F, Jasin M. Introduction of double-strand breaks into the genome of mouse cells by expression of a rare-cutting endonuclease. Mol Cell Biol. 1994;14(12):8096–106.

25. Cornu TI, Mussolino C, Bloom K, Cathomen T. Editing CCR5: A novel approach to HIV. In: Advances in Experimental Medicine and Biology. 2015. p. 117–30.

26. Hiroyuki S, Susumu K. New restriction endonucleases from Flavobacterium okeanokoites (FokI) and Micrococcus luteus (MluI). Gene. 1981;16(1–3):73–8.

27. Händel E, Cathomen T. Zinc-finger nuclease based genome surgery: it's all about specificity. Curr Gene Ther. 2011;11(1):28–37.

28. Mussolino C, Cathomen T. TALE nucleases: tailored genome engineering made easy. Curr Opin Biotechnol. 2012;23(5):644–50.

29. Zhang F, Huang L, Zhang F, Hu D, Wu W, Wang W, et al. Interacting Transcriptomes Revealing Molecular Mechanisms Underlying Mediated Broad Spectrum Resistance of Rice to Bacterial Blight. Plant Genome. 2015;8(3):0.

30. Boch J, Bonas U. *Xanthomonas* AvrBs3 Family-Type III Effectors: Discovery and Function. Annu Rev Phytopathol. 2010;48(1):419–36.

31. Perez EE, Wang J, Miller JC, Jouvenot Y, Kim KA, Liu O, et al. Establishment of HIV-1 resistance in CD4+ T cells by genome editing using zinc-finger nucleases. Nat Biotechnol. 2008;26(7):808–16.

32. Tebas P, Stein D, Tang WW, Frank I, Wang SQ, Lee G, et al. Gene Editing of CCR5 in Autologous CD4 T Cells of Persons Infected with HIV. n engl j med. 2014;37010370(10):901–10.

33. Meyer ED. Highly Efficient CCR5 Knockout in Human CD34+ Hematopoietic Stem Cells with Designer Nucleases. 2015.

34. Farzan M, Choe H, Vaca L, Martin K, Sun Y, Desjardins E, et al. A tyrosine-rich region in the N terminus of CCR5 is important for human immunodeficiency virus type 1 entry and mediates an association between gp120 and CCR5. J Virol. 1998;72(2):1160–4.

35. Hsu DC. JANEWAY'S IMMUNOBIOLOGY, 7TH EDITION. Shock. 2008 Jun;29(6):770.

36. Welsch, U., & Deller T. Lehrbuch Histologie: Unter Mitarbeit von Thomas Deller. Elsevier GmbH, Urban & Fischer Verlag; 2010.

37. Mohtashami M, Shah DK, Kianizad K, Awong G, Zúñiga-Pflücker JC. Induction of T-cell development by delta-like 4-expressing fibroblasts. Int Immunol. 2013;

38. Holmes R, Zuniga-Pflucker JC. The OP9-DL1 System: Generation of T-Lymphocytes from Embryonic or Hematopoietic Stem Cells In Vitro. Cold Spring Harb Protoc. 2009 Feb 1;2009(2):pdb.prot5156-pdb.prot5156.

39. Mumm JS, Kopan R. Notch signaling: from the outside in. Dev Biol. 2000;228(2):151–65.

40. Lehar SM, Bevan MJ. T cell development in culture. Immunity. 2002;17(6):689–92.

41. Allman D, Punt JA, Izon DJ, Aster JC, Pear WS. An invitation to T and more: Notch signaling in lymphopoiesis. Cell. 2002;109(2 SUPPL. 1):1–11.

42. Jaleco A, Blom B, Res P, Weijer K, Lanier L, Phillips J, et al. Fetal liver contains committed NK progenitors, but is not a site for development of CD34+ cells into T cells. J Immunol (Baltimore, Md 1950). 1997;159(2):694–702.

43. Hübner J, Hoseini SS, Suerth JD, Hoffmann D, Maluski M, Herbst J, et al. Generation of Genetically Engineered Precursor T-Cells From Human Umbilical Cord Blood Using an Optimized Alpharetroviral Vector Platform. Mol Ther. 2016 Jul 3;24(7):1216–26.

44. Reimann C, Six E, Dal-Cortivo L, Schiavo A, Appourchaux K, Lagresle-Peyrou C, et al. Human T-lymphoid progenitors generated in a feeder-cell-free delta-like-4 culture system promote T-cell reconstitution in NOD/SCID/γc-/- mice. Stem Cells. 2012;30(8):1771–80.

45. La Motte-Mohs RN. Induction of T-cell development from human cord blood hematopoietic stem cells by Delta-like 1 in vitro. Blood. 2005 Feb 15;105(4):1431–9.

46. Geissmann F, Jung S, Littman DR, Ajuebor MN, Flower RJ, Hannon R, et al. Blood Monocytes Consist of Two Principal Subsets with Distinct Migratory Properties. Immunity. 2003;19(1):71–82.

47. Forsyth RG, De Boeck G, Baelde JJ, Taminiau AH, Uyttendaele D, Roels H, et al. CD33+ CD14− Phenotype Is Characteristic of Multinuclear Osteoclast-Like Cells in Giant Cell Tumor of Bone. J Bone Miner Res. 2009;24(1):70–7.

48. Menetrier-caux BC, Montmain G, Dieu MC, Bain C, Favrot MC, Caux C, et al. Inhibition of the Differentiation of Dendritic Cells From CD34+Progenitors by Tumor Cells: Role of Interleukin-6 and Macrophage Colony-Stimulating Factor. Blood. 1998;92(12):4778–91.

49. Shibasaki T, Katayama N, Ohishi K, Fujieda A, Monma F, Nishii K, et al. IL-3 can not replace GM-CSF in inducing human monocytes to differentiate into Langerhans cell. Int J Oncol. 2007;30(3):549–55.

50. Korbie DJ, Mattick JS. Touchdown PCR for increased specificity and sensitivity in PCR amplification. Nat Protoc. 2008;3(9):13–5.

51. Parkinson MJ, Lilley DM. The junction-resolving enzyme T7 endonuclease I: quaternary structure and interaction with DNA. J Mol Biol. 1997;270(2):169–78.

52. Doyon Y, Choi VM, Xia DF, Vo TD, Gregory PD, Holmes MC. Transient cold shock enhances zinc-finger nuclease-mediated gene disruption. Nat Methods. 2010;7(6):459–60.

53. Dc W, Marrow B, Hao BQ, Shah AJ, Thiemann FT, Smogorzewska EM, et al. A functional comparison of CD34 + CD38- cells in cord blood and bone marrow. 2013;86(10):3745–53.

54. Pollard TD, Earnshaw WC. Cell Biology. 2nd ed. Spektrum Akademischer Verlag;

55. Lam YM, Chan YF, Chan LC, Ng RK. Histone deacetylase inhibitors induce leukemia gene expression in cord blood hematopoietic stem cells expanded ex vivo. Int J Hematol. 2016;

56. Kaushansky K, Lichtman M, Beutler E, Kipps T, Prchal J, Seligsohn U. Williams Hematology. McGraw-Hill Professional. 2010.

57. lonza.com [Internet]. 2016. Available from: http://www.lonza.com/products-services/bio-research/transfection/nucleofector-technology.aspx

58. Zhu J, Paul WE. Peripheral CD4 T cell differentiation regulated by networks of cytokines

and transcription factors. NIH. 2010;238(1):247–62.

59. Königs C, Pustowka A, Irving J, Kessel C, Klich K, Wegner V, et al. Peptide mimotopes selected with HIV-1-blocking monoclonal antibodies against CCR5 represent motifs specific for HIV-1 entry. Immunol Cell Biol. 2007;85(7):511–7.

60. bdbiosciences.com [Internet]. 2016. Available from: http://www.bdbiosciences.com/us/applications/research/b-cell-research/surface-markers/non-human-primates/apc-mouse-anti-human-cd195-3a9/p/560748

61. Reimer MK, Brange C, Rosendahl A. CCR8 signaling influences toll-like receptor 4 responses in human macrophages in inflammatory diseases. Clin Vaccine Immunol. 2011;18(12):2050–9.

62. Gombert M, Dieu-Nosjean M-C, Winterberg F, Bunemann E, Kubitza RC, Da Cunha L, et al. CCL1-CCR8 Interactions: An Axis Mediating the Recruitment of T Cells and Langerhans-Type Dendritic Cells to Sites of Atopic Skin Inflammation. J Immunol. 2005 Apr 15;174(8):5082–91.

63. Li L, Krymskaya L, Wang J, Henley J, Rao A, Cao L-F, et al. Genomic editing of the HIV-1 coreceptor CCR5 in adult hematopoietic stem and progenitor cells using zinc finger nucleases. Mol Ther. 2013;21(6):1259–69.

DANKSAGUNG

Herzlich bedanke ich mich bei Herrn Prof. Dr. Toni Cathomen und Herrn Prof. Dr. Ralf Wagner. Vielen Dank Herr Prof. Cathomen, dass Sie mir die Möglichkeit gegeben haben, bei Ihnen im CCI in Freiburg zu forschen. Ich habe in dieser Zeit sehr viel Methodik beigebracht bekommen und als Teil Ihres Teams die Strukturen im Labor kennen und schätzen gelernt. Für die Annahme meiner Arbeit und die Betreuung von Seiten der Universität Regensburg bedanke ich mich bei Ihnen Herr Prof. Wagner. Besonders Ihre Beratung bezüglich Form und Formalitäten war mir eine große Hilfe.

Besonderer Dank geht an Frau Dr. Tatjana Cornu. Die fachliche Betreuung und Zusammenarbeit mir Dir, Tatjana, in der AG Cornu habe ich sehr genossen. Herzlichen Dank, dass Du stets ein offenes Ohr hattest, wenn ich Probleme mit meinen Experimenten hatte und mir mit wertvollen Lösungsansätzen zur Seite gestanden hast. Die gemeinsamen Auswertungen der Versuche vor dem großen TV im Besprechungsraum haben mir immer viel Freude bereitet. Deine detaillierten Korrekturen und feinsinnigen Anmerkungen beim Schreiben dieser Arbeit haben mir enorm geholfen. Danke!

Das Erlernen aller Grundfertigkeiten vom Pipettieren, dem Benutzen der Zentrifuge über das Arbeiten in der Zellkultur bis hin zur Herstellung von RNA habe ich Frau Dr. Marianna Romito zu verdanken. Deine Hilfe im Labor, das Besprechen der Experimente und Deine Unterstützung als Freundin haben die Monate in Freiburg zu einer Zeit gemacht, an die ich mich wehmütig zurück erinnere. Ich hoffe, dass wir uns nie aus den Augen verlieren, denn so lustige, clevere und liebenswürdige Menschen wie Dich gibt es nur selten!

Einen sehr großen Teil meines Wissens über die Kultivierung von T-Zellen verdanke ich Herrn Dr. Jamal Alzubi. Du hast mir viel beigebracht über T-Zellen und über Durchflusszytometrie. Ohne Dich wäre diese Arbeit nicht möglich gewesen. Danke für Deine Geduld und das viele von Dir vermittelte Wissen!

Vielen herzlichen Dank für die Aufnahme ins Team und die schönen gemeinsamen Erlebnisse an Dr. Giando Turchiano, Dr. Valentina Pennucci, Melina el Gaz, Dr. Christien Bednarski, Ulf Gündisch, Nicola Bundschuh, Kenza Tauud, Ileana Bender, Nils Craig-Müller, Tafadzwa Mlambo, Dr. Maximilian Müller, Sandra Nitsch, Wladislaw Stroukov, Saskia König, Vivianne Dettmer, Emily Meyer, Simone Haas, Dr. Markus Hildenbeutel, Ilona Skatulla, Beate vom Hövel,

Petra Scheliga-Marschner, Beate Schmitt, Christine Reichenbach-Braun und Dr. Claudio Mussolino. Ihr alle wart einzigartig und wenn ich mich an meine Zeit in Freiburg erinnere, dann denke ich an Euch. Danke für diese tollen Monate!